CHAPTER 1 - INTRODUCTION AND THEORY

1.1 INTRODUCTION

In 1875, John Kerr[1] reported a birefringence in soft glass subjected to a strong electric field, and from that time the phenomenon of electric field-induced birefringence, subsequently called the electrooptic Kerr effect, the dc Kerr effect or simply the Kerr effect, has been an important means of investigating the polarization of molecules. The molar Kerr constant was defined by Otterbein[2] as

$$ {}_{\mathrm{m}}K = 6nV_{\mathrm{m}}\left[(n^2+2)^2(\varepsilon_{\mathrm{r}}+2)^2\right]^{-1}\left[(n_{\parallel}-n_{\perp})E^{-2}\right]_{E=0} \qquad (1.1) $$

where n is the isotropic refractive index, ε_r is the relative permittivity of the fluid, V_m is the molar volume and $n_{\parallel}$ and $n_{\perp}$ are the refractive indices parallel and perpendicular to the direction of the applied electric field, E. The dependence of the molar Kerr constant upon the gas density, due to interactions between molecules, is expressed in terms of the virial expansion[3]

$$ {}_{\mathrm{m}}K = A_{\mathrm{K}} + B_{\mathrm{K}}V_{\mathrm{m}}^{-1} + C_{\mathrm{K}}V_{\mathrm{m}}^{-2} + \ldots \qquad (1.2) $$

in which A_K, B_K and C_K are the Kerr first, second and third virial coefficients, respectively. In the absence of molecular interactions (i.e. in the limit of zero gas density), the molar Kerr constant is represented by A_K, and B_K measures the contribution due to pairs of interacting molecules. The Kerr third virial coefficient is assumed to be negligible for the low gas pressures used in this work.

Early researchers were principally concerned with measuring the Kerr effects of liquids, dilute solutions and vapours at single temperatures or pressures. From the 1960's, density- and temperature dependence studies of a range of molecules in the gas phase were performed by Buckingham and coworkers,[4-13] with further studies of this type being conducted by Ritchie and coworkers.[14-20] Although there have been several

other reported free-molecule Kerr-effect studies,[21-28] to date the electric properties of many important molecules, and how these are influenced by their constituent atoms, are unknown.

1.2 THEORY OF THE KERR EFFECT

Buckingham and Pople[29] derived a classical statistical mechanical theory describing the total polarization in molecules in a static electric field. For a molecule whose orientation and position can be described by the variable τ, its energy, $u(\tau,E)$, in an applied electric field, E_α, is given (using tensor notation) by the following expansion

$$\begin{aligned} u(\tau,E) &= u^0 - \mu_\alpha E_\alpha - \tfrac{1}{2}\alpha_{\alpha\beta}E_\alpha E_\beta - \tfrac{1}{6}\beta_{\alpha\beta\gamma}E_\alpha E_\beta E_\gamma \\ &\quad - \tfrac{1}{24}\gamma_{\alpha\beta\gamma\delta}E_\alpha E_\beta E_\gamma E_\delta - \cdots \end{aligned} \tag{1.3}$$

in which μ_α is the permanent electric dipole moment, $\alpha_{\alpha\beta}$ is the electric polarizability, $\beta_{\alpha\beta\gamma}$ is the first hyperpolarizability, and $\gamma_{\alpha\beta\gamma\delta}$ is the second hyperpolarizability. The tensors are symmetric in all suffixes. Thus, the total dipole moment of the molecule in an electric field is given by

$$\begin{aligned} m_\alpha &= -\frac{\partial u(\tau,E)}{\partial E_\alpha} \\ &= \mu_\alpha + \alpha_{\alpha\beta}E_\beta + \tfrac{1}{2}\beta_{\alpha\beta\gamma}E_\beta E_\gamma + \tfrac{1}{6}\gamma_{\alpha\beta\gamma\delta}E_\beta E_\gamma E_\delta + \cdots \end{aligned} \tag{1.4}$$

The differential polarizability, $\Pi_{\alpha\beta}$, is the subsequent increase in dipole moment per unit increase in the electric field, so that

$$\Pi_{\alpha\beta} = \frac{\partial m_\alpha}{\partial E_\beta} = \alpha_{\alpha\beta} + \beta_{\alpha\beta\gamma}E_\gamma + \tfrac{1}{2}\gamma_{\alpha\beta\gamma\delta}E_\gamma E_\delta + \ldots \tag{1.5}$$

with the two hyperpolarizability terms describing the nonlinear polarization that arises in strong fields. If molecular rotation is much slower than the period of oscillation of the light wave, then the differential polarizability difference for weak optical fields in directions $e^{\parallel}$ and $e^{\perp}$ is given by

$$\Pi(\tau,E) = \Pi_{\alpha\beta}(e^{\parallel}_{\alpha}e^{\parallel}_{\beta} - e^{\perp}_{\alpha}e^{\perp}_{\beta}) \tag{1.6}$$

where $e^{\parallel}_{\alpha}$ and $e^{\perp}_{\alpha}$ are the unit vectors parallel and perpendicular to the applied electric field. The expansion of Π in a power series in E leads to the first non-zero term being in E^2 and it can be shown that, in the limit of zero density,

$$A_{\mathrm{K}} = (N_{\mathrm{A}}/54\varepsilon_0)\left(\frac{\partial^2\overline{\Pi}}{\partial E^2}\right)_{E=0} \tag{1.7}$$

in which $\overline{\Pi}$ is the weighted average of the scalar Π, ε_0 is the permittivity of a vacuum and N_{A} is the Avogadro constant. Evaluation of the quantity

$$\left(\frac{\partial^2\overline{\Pi}}{\partial E^2}\right)_{E=0} = \left\langle\frac{\partial^2\Pi}{\partial E^2}\right\rangle - (kT)^{-1}\left\langle 2\left(\frac{\partial\Pi}{\partial E}\right)\left(\frac{\partial\mu}{\partial E}\right) + \Pi\left(\frac{\partial^2\mu}{\partial E^2}\right)\right\rangle + (kT)^{-2}\left\langle\Pi\left(\frac{\partial\mu}{\partial E}\right)^2\right\rangle \tag{1.8}$$

where $\langle X\rangle$ is the statistical average of $X(\tau,E)$ with $E=0$ leads to the final expression for the Kerr constant as

$$A_{\mathrm{K}} = (N_{\mathrm{A}}/81\varepsilon_0)\left\{\gamma^{\mathrm{K}} + (kT)^{-1}\left[(2/3)\mu\beta^{\mathrm{K}} + (3/10)\left(\alpha_{\alpha\beta}\alpha^0{}_{\alpha\beta} - 3\alpha\alpha^0\right)\right] + (3/10)(kT)^{-2}\mu^2(\alpha_{zz} - \alpha)\right\} \tag{1.9}$$

where the direction (− to +) of the dipole moment, μ, is fixed as the z-axis of the molecule, $\alpha^0{}_{\alpha\beta}$ is the zero-frequency or static polarizability, α now refers specifically to the mean optical-frequency or dynamic polarizability, and α^0 to the mean static polarizability. These latter two quantities are defined as

$$\alpha = \tfrac{1}{3}\left(\alpha_{xx} + \alpha_{yy} + \alpha_{zz}\right) \tag{1.10}$$

and $$\alpha^0 = \tfrac{1}{3}\left(\alpha^0{}_{xx} + \alpha^0{}_{yy} + \alpha^0{}_{zz}\right) \tag{1.11}$$

in terms of their molecule-fixed components. The quantities β^{K} and γ^{K} are the Kerr first and second hyperpolarizabilities, respectively. The temperature-independent term in

equation 1.9 is due to the electric-field induced distortion of the molecule and the other terms involve an orientational dependence. It is evident that for molecules lacking a permanent electric dipole moment this equation simplifies to

$$A_K = (N_A/81\varepsilon_0)\left\{\gamma^K + (3/10)(kT)^{-1}\left(\alpha_{\alpha\beta}\alpha^0_{\alpha\beta} - 3\alpha\alpha^0\right)\right\}. \tag{1.12}$$

For nondipolar molecules with C_{3v} or higher symmetry, this further reduces to

$$A_K = (N_A/405\varepsilon_0)\left\{5\gamma^K + (kT)^{-1}\left(\Delta\alpha\Delta\alpha^0\right)\right\} \tag{1.13}$$

where $\Delta\alpha = \alpha_{zz} - \alpha_{xx}$ and $\Delta\alpha^0 = \alpha^0_{zz} - \alpha^0_{xx}$ are the optical-frequency and static polarizability anisotropies, respectively. For species with spherical or tetrahedral symmetry, the orientation (and temperature dependent) term disappears to give

$$A_K = (N_A/81\varepsilon_0)\gamma^K. \tag{1.14}$$

1.3 THE KERR SECOND VIRIAL COEFFICIENT

The Kerr second virial coefficient represents the contribution of interactions between pairs of molecules to the Kerr effect. It has been shown that, for dipolar gases, the dominant contribution to B_K is that of the collision-induced polarizability[30] and

$$B_K = \frac{16\pi^2 N_A{}^2}{405kT(4\pi\varepsilon_0)^3}\left[\frac{\Delta\alpha\mu^4}{75(kT)^2}\left[\Delta\alpha^0 + \frac{\mu^2}{kT}\right] + 18\alpha^2\left(\alpha^0\right)^2 + \frac{12\alpha^2\alpha^0\mu^2}{kT} + \frac{2\alpha^2\mu^4}{(kT)^2}\right]\int_0^\infty R^{-6}\exp\left(-u^0_{12}/kT\right)R^2dR + \ldots \tag{1.15}$$

where R is the separation between the centres of the two interacting molecules and u^0_{12} is their nondipolar interaction energy. An expression for B_K has also been derived in terms of irreducible cluster polarizabilities for spherical top molecules by Dunmur and Jessup.[31]

1.4 QUANTUM MECHANICAL THEORY

The classical theory described in the preceding pages holds for most gases at normal temperatures, at which only the ground vibrational state is significantly populated and for which the rotational levels are closely spaced. In Buckingham's derivation of the quantum mechanical theory of the Kerr effect for diatomic molecules in the $^1\Sigma$ electronic ground state,[6] it was established that for those species with large rotational constants a quantum correction had to be included. If the excited vibrational levels are considered to have negligible populations, then

$$\begin{aligned} {}_{\mathrm{m}}K = (N_{\mathrm{A}}/81\varepsilon_0)\Big\{\gamma^{\mathrm{K}} + (kT)^{-1}\Big[\tfrac{2}{3}\mu\beta^{\mathrm{K}}\Big(1 - \tfrac{1}{3}\sigma_0 + \tfrac{2}{45}\sigma_0{}^2 + \ldots\Big) + \\ \tfrac{1}{5}\Delta\alpha\Delta\alpha^0\Big(1 - \sigma_0 + \tfrac{8}{15}\sigma_0{}^2 + \ldots\Big)\Big] + \\ \tfrac{1}{5}(kT)^{-2}\mu^2\Delta\alpha\Big(1 - \tfrac{5}{6}\sigma_0 + \tfrac{31}{90}\sigma_0{}^2 + \ldots\Big)\Big\} \end{aligned} \tag{1.16}$$

where $\sigma_0 = (hcB_0/kT)$ and B_0 is the rotational constant for the ground vibrational state. At temperatures above 200 K these quantum corrections are only significant for several hydrides, and for this work the classically derived equations are used.

1.5 THE ELECTRIC POLARIZABILITY

The polarizability, $\alpha_{\alpha\beta}$, is a second-rank tensor which describes the electric dipole moment induced in a molecule of any symmetry by an applied electric field. At an optical frequency, ω, sufficiently removed from the transition frequencies, ω_{kn}, so that there are no resonance effects, quantum mechanical perturbation theory can be used to express the polarizability as[32,33]

$$\alpha^{(n)}_{\alpha\beta}(-\omega;\omega) = \sum_k \frac{2\omega_{kn}}{\hbar\left(\omega_{kn}{}^2 - \omega^2\right)}\langle n|\mu_\alpha|k\rangle\langle k|\mu_\beta|n\rangle. \tag{1.17}$$

where n and k are electronic and vibrational states. The frequency dependence, or dispersion, of the polarizability and hyperpolarizabilities can be illustrated through consideration of the dipole moment oscillating at the polarization frequency, ω_σ, which is induced by electric fields of frequency ω_i.[33-36] This is expressed as

$$\begin{aligned}\mu_\alpha(\omega_\sigma) = {} & \alpha_{\alpha\beta}(-\omega_\sigma;\omega_\sigma)E_\beta(\omega_i) + \\ & \tfrac{1}{2}K(-\omega_\sigma;\omega_1,\omega_2)\beta_{\alpha\beta\gamma}(-\omega_\sigma;\omega_1,\omega_2)E_\beta(\omega_1)E_\gamma(\omega_2) + \\ & \tfrac{1}{6}K(-\omega_\sigma;\omega_1,\omega_2,\omega_3)\gamma_{\alpha\beta\gamma\delta}(-\omega_\sigma;\omega_1,\omega_2,\omega_3)E_\beta(\omega_1)E_\gamma(\omega_2)E_\delta(\omega_3) + \ldots\end{aligned} \tag{1.18}$$

Positive frequencies arise for photons being absorbed and negative frequencies for photons being emitted. They sum to zero for any optical process. The values of the numbers $K(-\omega_\sigma;\omega_1,\omega_2)$ and $K(-\omega_\sigma;\omega_1,\omega_2,\omega_3)$ depend upon the presence of zero and repeated frequencies for the set $\omega_1,\omega_2,\omega_3\ldots$[36] In this work, all dynamic properties are reported at a frequency corresponding to a wavelength of 632.8 nm, unless otherwise stated.

The polarizability has also been reported to possess a limited temperature and pressure dependence. Hohm and Kerl[37] have investigated several molecules and found that the polarizability generally varies by less than 0.2% over a range of 150 K. The pressure dependence has been explored by Buckingham and Graham[38] by means of a virial expansion in the molar refractivity, and virial refractivity coefficients have been determined for several molecules. However, these contributions are also small and the classical theory of the Kerr effect assumes that the polarizability is independent of both temperature and pressure.

The mean polarizability at optical frequencies can be determined from refractive index measurements and the Lorentz-Lorenz equation[39,40]

$$\left(n^2-1\right)\left(n^2+2\right)^{-1}V_m = N_A\alpha/3\varepsilon_0 \tag{1.19}$$

where the right-hand term is also referred to as the molar refractivity, R_m. Optical-frequency polarizabilities measured for different physical states have been found to agree

to within 1% [41] and, in general, liquid- and solution-phase refractivities are utilised to determine free-molecule polarizabilities. Studies of the dispersion in the polarizability allow evaluation of the electronic component of the static polarizability, α^0_{elec}, and, if the vibrational component, α^0_{vib}, can be estimated from the intensities of the infrared active bands,[42] the static polarizability can be determined. Alternatively, the relative permittivity of a fluid can give the static polarizability directly through the Clausius-Mossotti relation[43]

$$(\varepsilon_r - 1)(\varepsilon_r + 2)^{-1} = (N_A/3\varepsilon_0 V_m)\left[\alpha^0 + \left(\mu^2/3kT\right)\right]. \qquad (1.20)$$

Such measurements have in the past[44,45] been performed on a large number of solutions and gases. However, the dipole moments obtained from some of these studies are not as precise as those that have been measured using microwave spectroscopy. The long extrapolations against T^{-1} that are required in analyses of these measurements are also uncertain and, therefore, the reliability of static polarizabilities determined from dielectric polarization measurements is often not high.

More recently, accurate optical-frequency and static electric polarizabilities have been determined from a combination of molar refractivities and photoabsorption oscillator strengths.[46] Analysis of these leads to the dipole oscillator strength distributions, which provide information on a number of dipole properties, including the dipole sums or Cauchy moments. These Cauchy moments, $S(-2k-2)$, where the value of the index k corresponds to a particular molecular property, describe the dispersion over small ranges of ω, and are given by the expansion

$$\alpha_{(\omega)} = \sum_{k=0}^{\infty} S(-2k-2)\omega^{2k} \qquad (1.21)$$

in which $S(-2)$ is the electronic contribution to the mean static polarizability.

1.6 THEORY OF RAYLEIGH LIGHT SCATTERING

When plane-polarized light is incident upon a molecule in the absence of a static electric field, an oscillating dipole is induced in the molecule by the electromagnetic wave. The component of light scattered at 90° to the electric field vector of the light is, in general, depolarized. If an analyzer is positioned perpendicular to the electric field vector, then the steradiance, or mean rate of radiation per unit solid angle, is equal to [47]

$$S_0 = I_0(4\pi\varepsilon_0)^{-2}(2\pi\omega/c)^4\left(\alpha_{\alpha\beta}q_\alpha e_\beta\right)^2 \tag{1.22}$$

where I_0 is the intensity, ω is the frequency and e_β is the unit vector in the direction of the plane of polarization of the incident light. The unit vector in the direction of the transmission axis of the analyzer is represented by q_α. When a molecule-fixed axis system is chosen, the components of $\alpha_{\alpha\beta}$ are independent of the molecular orientation and the mean steradiance is found by averaging over all molecular orientations, such that

$$\langle S_0\rangle = I_0(4\pi\varepsilon_0)^{-2}(2\pi\omega/c)^4(\alpha^2/5)\left[3\kappa^2+\left(5+\kappa^2\right)\cos^2\theta\right] \tag{1.23}$$

where θ is the angle between the vectors e_β and q_α. The polarizability anisotropy parameter, κ, is related to the molecular polarizability components by

$$\kappa^2 = \left(3\alpha_{\alpha\beta}\alpha_{\alpha\beta} - \alpha_{\alpha\alpha}\alpha_{\beta\beta}\right)/2\alpha_{\alpha\alpha}\alpha_{\beta\beta}. \tag{1.24}$$

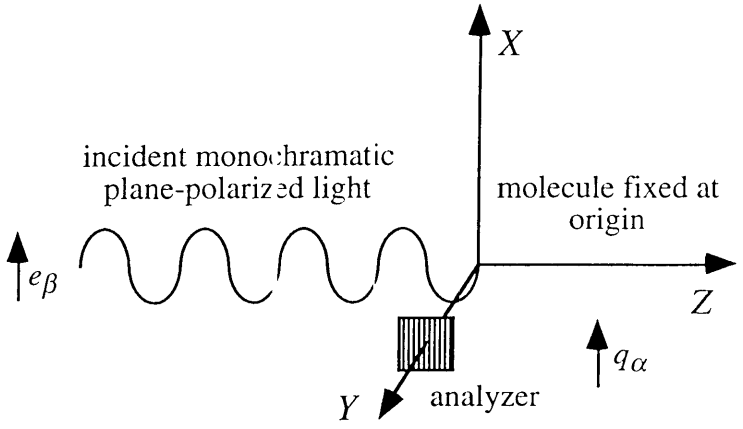

Figure 1.1 Scattering geometry for 90° Rayleigh scattered light.

The hyperpolarizabilities give rise to such nonlinear optical phenomena as hyper-Rayleigh and hyper-Raman scattering. However, this higher order light-scattering is insignificant compared to the first order Rayleigh light-scattering, especially for the low powered lasers used for all of the measurements referred to in this thesis. The measurement of the steradiance that corresponds to horizontally scattered light, I_h^V, and the light scattered vertically to the incident beam, I_v^V, gives the depolarization ratio, ρ_0, where

$$\rho_0 = I_h^V / I_v^V = 3\kappa^2 / \left(5 + 4\kappa^2\right) \tag{1.25}$$

or, upon rearragement,

$$\kappa^2 = 5\rho_0 / (3 - 4\rho_0). \tag{1.26}$$

The visible wavelengths used in light scattering experiments are far removed from any electronic transitions, but vibrational Raman lines are present and must be filtered out for weakly anisotropic molecules. The scattered light retained thus consists of the central Cabannes line and the rotational Raman lines. In the quantum mechanical treatment of light scattering, frequency factors are derived for the O, Q and S branches of the rotational Raman spectrum.[47] As with the Kerr effect, these quantum corrections are only significant for very small molecules. For the molecules investigated in conjunction with the Kerr-effect studies reported in this thesis, the classical Rayleigh light-scattering theory is assumed to be applicable when the vibrational Raman lines are excluded.

Mean polarizabilities at optical frequencies have also been obtained from the Rayleigh light-scattering experiment through the relationship [48]

$$\alpha = \alpha(\mathrm{Ar}) \left[\left(I_v^V / I_v^V(\mathrm{Ar}) \right) \left(1 - (4\rho_0/3)\right) \right]^{\frac{1}{2}} \tag{1.27}$$

where $\alpha(\mathrm{Ar})$ is the mean polarizability of argon and $I_v^V(\mathrm{Ar})$ is the vertically polarized scattered-light intensity for argon.

1.7 BOND ADDITIVITY SCHEMES FOR THE POLARIZABILITY

The mean polarizability is known to be an approximately additive scalar property of a molecule's constituent bonds and functional groups. For this reason, a variety of additivity schemes have been suggested in the past for correlating and predicting experimental results. Endeavours in this area have been summarized in the review by Le Fèvre.[49] Most of these schemes have only a limited application as they make no allowance for environment or group interaction. An improvement on these is the interacting segment model proposed by Miller, Orr and Ward,[50] which uses "dressed" tensors to describe the electrostatic interactions that modify the "bare" or point electric tensors. This procedure has been used for the fluoromethanes and chloromethanes[51] to estimate reasonably accurate dipole moments, polarizabilities and hyperpolarizabilities. Mean polarizabilities have also been calculated for several hundred compounds by Miller using atomic hybrid and group methods.[52] and a semi-empirical approach involving modified dipole tensors.[53]

1.8 COMPUTATIONAL METHODS

There has long been great interest in using quantum mechanical procedures to determine mean and anisotropic polarizabilities, and this has been dramatically increased in the recent literature.[54,55] With the advent of high speed, powerful computers the earlier semi-empirical results are being superseded by an abundance of accurate ab initio calculations for many systems. However, these are still limited for larger and more chemically interesting molecules and this field is still in a developmental stage as the effects on the calculations of basis set size, electron correlation, dispersion and vibrational and rotational averaging become better understood.

1.9 MOLECULAR HYPERPOLARIZABILITIES

The first and second hyperpolarizabilities are third- and fourth-rank tensors, respectively, which describe the nonlinear polarization of the molecule. These tensors contain 3^n elements, where n is the order of the tensor, but symmetry simplifies their specifications in terms of their unique elements. These terms are known for both the static and optical-frequency hyperpolarizabilities,[32] in which the symmetry with respect to the interchange of suffixes does not occur. However, the approximation is considered reasonable if the optical frequency is far removed from the absorption frequencies.[56]

All molecules have a non-zero mean second hyperpolarizability, although the mean first hyperpolarizability is zero for molecules with a centre of inversion. The presence of lower symmetry introduces other non-zero terms, and the numbers of independent constants required to specify the static polarizability and hyperpolarizability tensors are given in Table 1.1.[33,34,56]

In terms of the frequency-dependence formalism of equation 1.18, the Kerr first and second hyperpolarizabilities are defined as [33]

$$\beta^{K} = (3/10)\left(3\beta_{\alpha z\alpha}(-\omega;\omega,0) - \beta_{\alpha\alpha z}(-\omega;\omega,0)\right) \tag{1.28}$$

and $$\gamma^{K} = (1/10)\left(3\gamma_{\alpha\beta\alpha\beta}(-\omega;\omega,0,0) - \gamma_{\alpha\alpha\beta\beta}(-\omega;\omega,0,0)\right). \tag{1.29}$$

The first and second hyperpolarizabilities also arise in various other nonlinear optical processes and values have been reported for several of these other phenomena.[54] Many of these are from electric field-induced second harmonic generation (ESHG or EFISH), in which a pulsed laser propagated transversely to the electrostatic field generates a second harmonic signal whose magnitude is related to the hyperpolarizabilities. A comparison of the temperature dependence of the measurements on the sample gas with those of a standard allows the separation of $\beta(-2\omega;\omega,\omega)$ and $\gamma(-2\omega;0,\omega,\omega)$. Other results which have been reported arise from third harmonic

Table 1.1 Non-zero elements of the static polarizability and hyperpolarizabilities for compounds investigated in this work

Symmetry Group	Investigated Examples	$\alpha_{\alpha\beta}$ non-zero components	$\beta_{\alpha\beta\gamma}$ number of unique non-zero components	$\gamma_{\alpha\beta\gamma\delta}$ number of unique non-zero components
T_d	tetrabromomethane	$\alpha_{xx} = \alpha_{yy} = \alpha_{zz}$	1	2
$D_{\infty h}$ [a]	dimethylacetylene	$\alpha_{xx} = \alpha_{yy}$; α_{zz}	0	3
$C_{\infty v}$	methylacetylene	$\alpha_{xx} = \alpha_{yy}$; α_{zz}	2	3
C_{3v}	ammonia, trimethylamine,[a] bromomethane and tribromomethane	$\alpha_{xx} = \alpha_{yy}$; α_{zz}	3	4
D_{2h}	1,4-difluoro- and 1,2,4,5-tetrafluoro-benzene	α_{xx} ; α_{yy} ; α_{zz}	0	6
C_{2v}	1,2-difluoro-, 1,3-difluoro- and 1,2,3,5-tetrafluoro-benzene, dibromomethane and pyridine	α_{xx} ; α_{yy} ; α_{zz}	3	6
C_s [a]	methylamine, dimethylamine and fluoroethane	α_{xx} ; α_{yy} ; α_{zz} ; α_{xz}	6	9

a) In the minimum-energy conformation of the molecule.

generation (THG); various wave-mixing experiments; coherent anti-Stokes Raman scattering and the ac- or optical-Kerr effect, which is analogous to the Kerr effect, but uses the electric field vector of high-powered laser radiation to induce the birefringence.

The derived coefficients $K(-\omega_\sigma;\omega_1,\omega_2)$ and $K(-\omega_\sigma;\omega_1,\omega_2,\omega_3)$ for these processes depend on the various frequencies involved and their values are given in Table 1.2.[57] The electronic contributions of the hyperpolarizabilities for each process converge in the limit of zero frequency.[33,34,35,58]

As molecular size increases both the electronic and vibrational hyperpolarizabilities tend to increase in magnitude, although these two contributions are difficult to separate for most molecules, due to a lack of information about the dispersion and the often large uncertainties associated with the experimental results. Elliott and Ward[58] have analyzed the vibrational hyperpolarizability for several nonlinear optical processes in terms of the applied field frequencies. The vibrational contribution tends to increase in the order THG < ESHG < degenerate four-wave mixing < ac Kerr effect and Kerr effect.[54]

There has been considerable interest in developing schemes for predicting the hyperpolarizabilities,[50,51] analogous to the additivity models used for the polarizability. Bond-additivity methods work well for γ, which transforms as a scalar quantity. However, there has been less success using this approach for β, whose experimental observable transforms as a vector, and, as yet, no model is satisfactory for the majority of systems.

Computational methods are being used far more frequently to determine both static and optical-frequency hyperpolarizabilities. Impressive results have been achieved for several small systems using various ab initio methods.[54,55] Unfortunately, these highest levels of theory are at present still not practical for even medium-size polyatomic molecules. This area has, therefore, remained the province of semi-empirical methods and self-consistent field (SCF) calculations, with the degree of accuracy of the results being generally low.

Table 1.2 Hyperpolarizabilities for various nonlinear optical processes

Process	$-\omega_\sigma$	ω_1	ω_2	ω_3	$K(-\omega_\sigma;\omega_1,\omega_2,\omega_3)$ [a]
First hyperpolarizability					
static	0	0	0	–	1
Kerr effect	$-\omega$	0	ω	–	2
second harmonic generation	-2ω	ω	ω	–	1/2
Second hyperpolarizability					
static	0	0	0	0	1
Kerr effect	$-\omega$	ω	0	0	3
second harmonic generation	-2ω	0	ω	ω	3/2
third harmonic generation	-3ω	ω	ω	ω	1/4
ac Kerr effect	$-\omega_1$	ω_1	ω_2	$-\omega_2$	3/2
degenerate four -wave mixing	$-\omega$	ω	$-\omega$	ω	3/4

a) The coefficients $K(-\omega_\sigma;\omega_1,\omega_2)$ and $K(-\omega_\sigma;\omega_1,\omega_2,\omega_3)$ are calculated from[35]

$$K(-\omega_\sigma;\omega_1,\omega_2,\omega_3) = 2^m \times D$$

where m equals the number of non-zero polarization frequencies, ω_σ, (which is equal to one in all dynamic cases) minus the number of non-zero field frequencies in the set $\omega_1,\omega_2,\omega_3$. D is the number of distinct permutations of the frequency labels $\omega_1,\omega_2,\omega_3$, with ω being distinguishable from $-\omega$.

1.10 DISCUSSION

The Kerr effect has proven to be a prolific source of information on the polarization of molecules. However, much of the earlier work involved measurements on solutions, and the results from these studies are influenced by local-field effects and not applicable to non-interacting systems. Investigations of the density- and temperature dependences of the Kerr effect of gases and the vapours of liquids are required to determine the polarizabilities and hyperpolarizabilities of free molecules. Many of the previous studies of this type were performed on reasonably small molecules.

This work is principally concerned with investigations of larger and more chemically interesting species. Density dependence measurements were performed in most of these studies, allowing the determination of values of both A_K and B_K for all but the least volatile species. The method of analysis of the temperature dependence of A_K in each study depended on the symmetry of the molecule being investigated. As has already been shown, this generally required the separation of a temperature-independent term from terms dependent on T^{-1} and T^{-2}. The combination of these results with other data then enabled the determination of the polarizabilities and hyperpolarizabilities, the primary focus of this thesis. A number of assumptions have been made in the earlier studies regarding the contributions of the Kerr first and second hyperpolarizabilities and the static polarizability anisotropy to A_K. It was also an aim of this work to test the validity of these assumptions by obtaining reliable values of these quantities for a range of polyatomic molecules. The determination of the polarizabilities of those molecules with C_s symmetry in their equilibrium conformations required data obtained from ab initio calculations. The relevant theory for this procedure, and the effects of the accuracy of the calculations, are discussed in the appropriate chapters of this thesis.

A number of the studies documented in the following chapters are an extension of, or were made in conjunction with, other work. The measurements on the bromomethanes, fluoroethane and the fluorobenzenes are continuations of earlier studies of the fluoromethanes[7], chloromethanes[11], other halogenoethanes[20] and the

fluorobenzenes.[15,16] This has enabled systematic examinations of the effects of halogen atoms on the polarizabilities and hyperpolarizabilities of aliphatic and aromatic molecules. The studies of the methylamines, methylacetylenes and pyridine complement recent investigations of the Rayleigh light scattering,[20] Cotton-Mouton effect[59,60] and electric field-gradient induced birefringence[61] of these species, undertaken in this laboratory.

The following chapters detail, first, the apparatus used to carry out the Kerr-effect measurements, and then present the results and discussions for the various molecules that were investigated.

1.11 REFERENCES

1 Kerr, J., *Phil. Mag.*, **50**, 337, 446 (1875).

2 Otterbein, G., *Phys. Z.*, **35**, 249 (1934).

3 Buckingham, A.D., *Proc. Phys. Soc. A*, **68**, 910 (1955).

4 Boyle, L.L., Buckingham, A.D., Disch, R.L. and Dunmur, D.A., *J. Chem. Phys.*, **45**, 1318 (1966).

5 Buckingham, A.D. and Dunmur, D.A., *Trans. Faraday Soc.*, **64**, 1776 (1968).

6 Buckingham, A.D. and Orr, B.J., *Proc. Roy. Soc. A*, **305**, 259 (1968).

7 Buckingham, A.D. and Orr, B.J., *Trans. Faraday Soc.*, **65**, 673 (1969).

8 Buckingham, A.D., Bogaard, M.P., Dunmur, D.A., Hobbs, C.P. and Orr, B.J., *Trans. Faraday Soc.*, **66**, 1548 (1970).

9 Buckingham, A.D. and Sutter, H., *J. Chem. Phys.*, **64**, 364 (1976).

10 Bogaard, M.P., Buckingham, A.D. and Ritchie, G.L.D., *Mol. Phys.*, **18**, 575 (1970).

11 Bogaard, M.P., Orr, B.J., Buckingham, A.D. and Ritchie, G.L.D., *J. Chem. Soc., Faraday Trans. 2*, **74**, 1573 (1978).

12 Bogaard, M.P., Orr, B.J., Buckingham, A.D. and Ritchie, G.L.D., *J. Chem. Soc., Faraday Trans. 2*, **77**, 1547 (1981).

13 Bogaard, M.P., Buckingham, A.D. and Ritchie, G.L.D., *Chem. Phys. Lett.*, **90**, 183 (1982).

14 Gentle, I.R., Laver, D.R. and Ritchie, G.L.D., *J. Phys. Chem.*, **93**, 3035 (1989).

15 Gentle, I.R. and Ritchie, G.L.D., *J. Phys. Chem.*, **93**, 7740 (1989).

16 Gentle, I.R., Hesling, M.R. and Ritchie, G.L.D., *J. Phys. Chem.*, **94**, 1844 (1990).

17 Gentle, I.R., Laver, D.R. and Ritchie, G.L.D., *J. Phys. Chem.*, **94**, 3434 (1990).

18 Gentle, I.R., Halliburton, B.W. and Ritchie, G.L.D., unpublished results.

19 Gentle, I.R., Ritchie, G.L.D. and Watson, J.N., unpublished results.

20 Ritchie, G.L.D. and Stankey R., unpublished results.

21 Burnham, A.K., Buxton, L.W. and Flygare, W.H., *J. Chem. Phys.*, **67**, 4990 (1977).

22 Dunmur, D.A., Hunt, D.C. and Jessup, N.E., *Mol. Phys.*, **37**, 713 (1979).

23 Tammer, R. and Hüttner, W., *Chem. Phys.*, **146**, 155 (1990).

24 Tammer, R. and Hüttner, W., *Chem. Phys.*, **168**, 151 (1992).

25 Tammer, R., Löblein, K., Peting, K.H. and Hüttner, W., *Chem. Phys.*, **168**, 151 (1992).

26 Shelton, D.P. and Rugar, B., *Chem. Phys. Lett.*, **201**, 364 (1993).

27 Tammer, R. and Hüttner, W., *Mol. Phys.*, **83**, 579 (1994).

28 Shelton, D.P. and Palubinskas, J.J., *J. Chem. Phys.*, **104**, 2482 (1996).

29 Buckingham, A.D. and Pople, J.A., *Proc. Phys. Soc. A*, **68**, 905 (1955).

30 Buckingham, A.D., Galwas, P.A. and Liu Fan-Chen, *J. Mol. Struct.*, **100**, 3 (1983).

31 Dunmur, D.A. and Jessup, N.E., *Mol. Phys.*, **37**, 697 (1979).

32 Buckingham, A.D., *Permanent and Induced Molecular Moments and Long-Range Intermolecular Forces* in *Advances in Chemical Physics*, Vol. 12 (J.O. Hirschfelder editor), (Interscience, New York, 1967).

33 Bogaard, M.P. and Orr, B.J., *Electric Dipole Polarizabilities of Atoms and Molecules* in *MTP International Review of Science, Physical Chemistry, Series 2*, Vol. 2 (A.D. Buckingham editor), (Butterworths, London, 1975).

34 Buckingham, A.D. and Orr, B.J., *Quart. Rev.*, **21**, 195 (1967).

35 Orr, B.J. and Ward, J.F., *Mol. Phys.*, **20**, 513 (1971).

36 Ward, J.F., *Rev. Mod. Phys.*, **37**, 1 (1965).

37 Hohm, U. and Kerl, K., *Mol. Phys.*, **58**, 541 (1986).

38 Buckingham, A.D. and Graham, C., *Proc. R. Soc. London A*, **336**, 275 (1974).

39 Lorentz, H.A., *Ann. Phys.*, **9**, 641 (1880).

40 Lorenz, L., *Ann. Phys.*, **11**, 70 (1880).

41 Bogaard, M.P., Buckingham, A.D., Pierens, R.K. and White, A.H., *J. Chem. Soc., Faraday Trans. I*, **74**, 3008 (1978).

42 Bishop, D.M. and Cheung, L.M., *J. Phys. Chem. Ref. Data*, **11**, 119 (1982).

43 Debye, P., *Z. Phys.*, **13**, 97 (1912).

44 Le Fèvre, R.J.W., *Dipole Moments* (Methuen, London, 1953).

45 Landolt-Börnstein, *Zahlenwerte und Funktionen,* Band II, Teil 6 (Springer, Berlin, 1959).

46 Burton, G.R., Chan, W.F. Cooper, G., Brion, C.E., Kumar, A. and Meath, W.J., *Can. J. Chem.*, **71**, 341 (1993).

47 Bridge, N.J. and Buckingham, A.D., *Proc. Roy. Soc. A*, **295**, 334 (1966).

48 Alms, G.R., Burnham, A.K. and Flygare, W.H., *J. Chem. Phys.*, **63,** 3321 (1975).

49 Le Fèvre, R.J.W., *Advances in Physical Organic Chemistry*, Vol. 3 (V. Gold editor), (Chemical Society, London, 1965).

50 Miller, C.K., Orr, B.J. and Ward, J.F., *J. Chem. Phys.*, **67,** 2109 (1977).

51 Miller, C.K., Orr, B.J. and Ward, J.F., *J. Chem. Phys.*, **74,** 4858 (1981).

52 Miller, K.J., *J. Am. Chem. Soc.*, **112**, 8533 (1990).

53 Miller, K.J., *J. Am. Chem. Soc.*, **112**, 8543 (1990).

54 Shelton, D.P. and Rice, J.E , *Chem. Rev.*, **94,** 3 (1994).

55 Bishop, D.M., *Aspects of Non-Linear-Optical Calculations* in *Advances in Quantum Chemistry*, Vol. 25 (Academic Press, London, 1994).

56 Buckingham, A.D. and Stephen, M.J., *Trans. Faraday Soc.*, **53**, 884 (1957).

57 Butcher, P.N. and Cotter, D., *The Elements of Nonlinear Optics* in *Cambridge Studies in Modern Optics 9* (Cambridge University Press, Cambridge, 1990).

58 Elliott, D.S. and Ward, J.F., *Mol. Phys.*, **51,** 45 (1984).

59 Coonan, M.H., *Ph.D. Thesis* (University of New England, 1995).

60 Lamb, D.W. and Ritchie, G.L.D., unpublished results.

61 Watson, J.N., *Ph.D. Thesis* (University of New England, 1994).

CHAPTER 2 - EXPERIMENTAL DETAILS

2.1 INTRODUCTION

The basic apparatus used to carry out the Kerr-effect measurements, reported in the following chapters, has been described elsewhere.[1] However, several modifications have been made in an effort both to improve the sensitivity of the apparatus and the accuracy of the measurements, and also to widen the range of chemical species which could be investigated. These improvements will be discussed in greater detail here. A description of the procedure for recording measurements is also included.

As noted in the preceding chapter, the analysis of the electrical properties of the molecules of interest required data from other sources, in particular, the Rayleigh light-scattering experiment. Several of the light-scattering measurements cited here were performed by the author. A description of the Rayleigh light scattering apparatus is, therefore, also included.

2.2 KERR-EFFECT APPARATUS

The optical train and electronics for the Kerr-effect apparatus are shown in Figure 2.1. A plane-polarized He-Ne laser of either 2 mW or 10 mW power was used as the radiation source. The light first traversed an uncoated Glan-Taylor polarizing prism (Karl Lambrecht Corporation) with an extinction coefficient of $<10^{-5}$. The polarizer prism was mounted in cork inside a brass cylinder, with the transmission axis orientated at $\pi/4$ to the electrodes of the gas Kerr cell. This was then wedged inside another brass cylinder, which had a brass arm of known length attached with a spring-pressure driven micrometer at the other end to allow accurate rotations of the polarizer to be made. The analyzer consisted of an identical arrangement, but with the transmission axis crossed with respect to that of the polarizer.

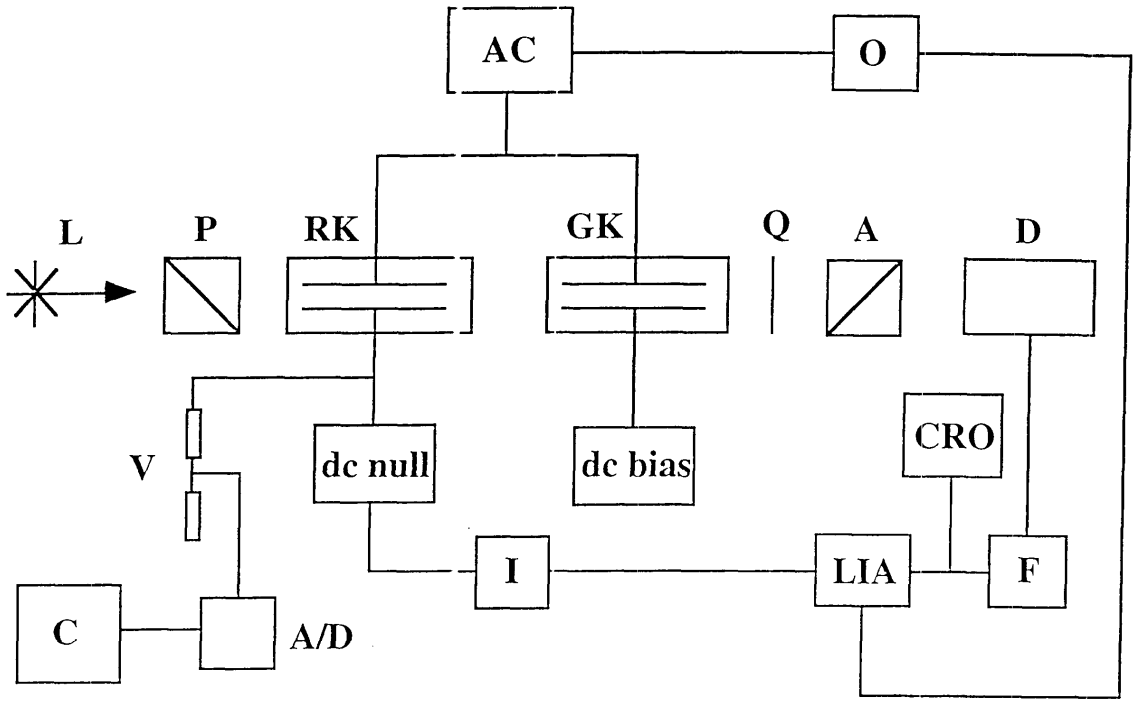

Figure 2.1 Apparatus for the measurement of the Kerr effect in gases and vapours.

L, laser; **P**, polarizer; **RK**, reference Kerr cell; **GK**, gas Kerr cell; **Q**, quarterwave plate; **A**, analyzer; **D**, detector; **AC**, ac voltage power supply; **O**, oscillator; **dc bias**, dc voltage power supply for gas Kerr cell; **dc null**, dc voltage power supply for reference Kerr cell; **F**, filter; **CRO**, oscilloscope; **LIA**, lock-in amplifier; **I**, integrator; **V**, voltage divider; **A/D**, analog-to-digital converter; **C**, microcomputer

The gas sample was contained within the new gas Kerr cell, which will be described in detail, together with the gas-handling system, later. As with Gentle's apparatus, a glass-mounted 19 mm diameter close-tolerance quarterwave plate (F. Wiggins and Sons Ltd.) was mounted between Viton O-rings in a brass stand. The original reference Kerr cell, constructed by Vrbancich,[2,3] was retained. In this, parallel brass electrodes were separated by three glass spacers arranged in a tripod configuration. This assembly was securely mounted in a brass cylinder with fused quartz optical windows (Suprasil 1, Heraeus Quarzshmelze) seated on Viton O-rings. These displayed

a low retardance (typically 1.5×10^{-4} radians per window pair) and negligible long term drift. The reference Kerr cell was filled with cyclohexane, which had been twice distilled, dried over sodium wire and then passed through 0.22 μm membrane filters. Periodically throughout the course of these measurements, the reference Kerr cell was refilled and on each occasion the cell was left for sufficient time for the signal noise to reach typical background levels before use.

After each refill of the cyclohexane reservoir, as well as periodically during measurements, the reference Kerr cell was calibrated using a procedure based on the Sénarmont method,[4] as described by Gentle.[1] This involved applying a large dc voltage to one electrode of the reference Kerr cell, with the other electrode being grounded, and the use of a Faraday coil to provide signal modulation. The birefringence was then nulled using a second calibrated Faraday coil, with the applied dc voltage being recorded. Repeated averaging gave a typical reference Kerr cell constant, k_2, of $(2.665 \pm 0.014) \times 10^{-11}$ rad V^{-2}. As has been previously noted,[1] the reference Kerr cell was found to be extremely stable over long periods.

All optical components were mounted on, and clamped to, a steel H-section beam. The optical rail and frame were insulated by neoprene rubber, which kept vibrations to a minimum. This arrangement has been described by Vrbancich[2] and was used without modification.

The electronics system was similar to that described by Gentle.[1] A Model 141 signal generator (BWD Electronics Pty Ltd.), operating at 512 Hz, supplied a sinusoidal reference voltage. At this frequency there was no interference from the mains harmonics and distortion, $1/f$ noise and signal power loss were all kept to acceptable levels. The required stable high voltage power supply consisted of a 150 W Mosfet-type power amplifier and a custom-built transformer (Ferguson Transformers). Although this unit was capable of generating up to 10 kV, the measurements reported in the following chapters were all recorded using modulation voltages of 0.4 to 2.5 kV rms. The very low vapour pressures and reactive natures of many of the species investigated resulted in

low breakdown potentials, which often led to the use of small bias and modulation voltages.

A Fluke 410B 0-10 kV dc power supply provided the bias voltage for the gas Kerr cell. The calibration of this power supply, using a highly accurate voltage divider, had previously[1] been found to be within 0.15% of the front panel readings. However, deterioration due to long service and the subsequent repairs were found to alter the calibration. The front panel settings were remeasured using a Fluke 80K-6 high-voltage probe and a Fluke 8810A digital multimeter (± 0.06% accuracy). Although the voltage probe had an absolute accuracy of only ± 1%, the repeatability of the voltage calibration was determined to be within 0.03% over a period of 10 months. Although the new voltages were found to differ from the original calibrated voltages by less than 0.3%, they were stable at these new values and were used for the measurements on the bromomethanes, methylacetylenes and fluoroethane.

The Fluke dc power supply was connected through a relay to the annunciator output of an Apple IIe microcomputer. This allowed for the automatic operation of the dc power supply through the software, while manual control could easily be exercised by disconnecting the interface.

The signal generator provided the reference signal for a lock-in amplifier (Ithaco Dynatrac 393), which was connected to a filter (Ithaco 4302, dual 24 dB/octave). This filter passed only modulated signals between 315 and 800 Hz. The internal earth of the lock-in amplifier was isolated and the signal path was grounded externally to prevent ground loops.

The replacement of the Kepco BOP-1000M, which was used by previous researchers,[1,5,6] by the Fluke 410B dc power supply necessitated the modification of the detection system. This new configuration is shown in Figure 2.2. The integrator used by Gentle to provide the nulling voltage for the reference Kerr cell (based on an LF356 FET amplifier and capable of fast tracking with minimal overshoot) was connected to the optoisolator circuit shown. The 3 kV of electrical insulation that this provided protected the integrator from the high voltage side of the circuit. Nulling voltages of up to 1000 V

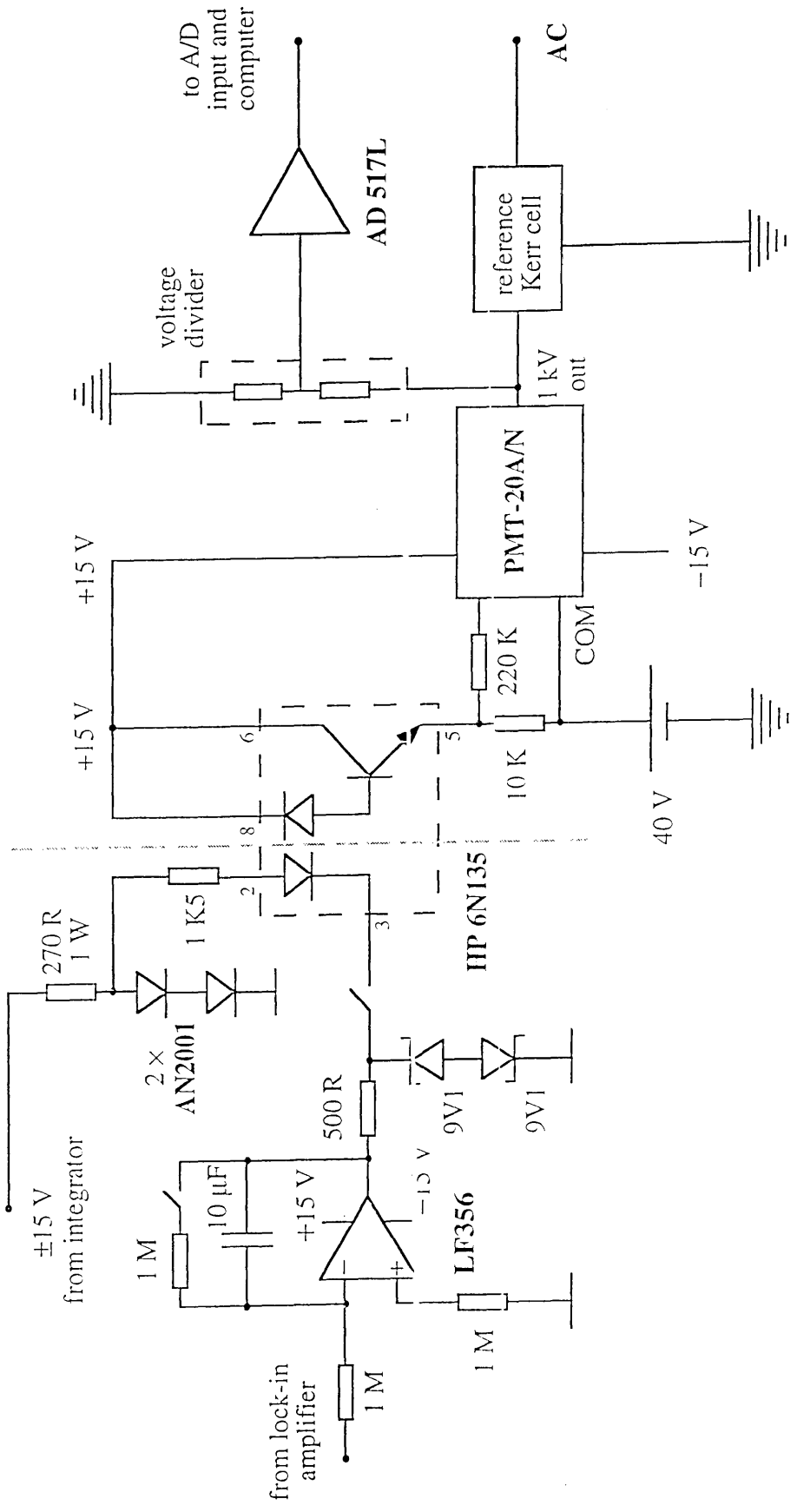

Figure 2.2 Nulling dc-voltage control circuitry.

LF356, integrator; **IIP 6N135**, optoisolator; **PMT-20A/N**, 1000 V programmable power supply; **AC**, ac voltage power supply; **AN2001**, diodes; **AD 517L**, buffer amplifier

were supplied by a Bertan PMT-20A/N power supply, although in practice the typical nulling voltages used were much smaller than this maximum value. A calibrated voltage divider and buffer amplifier allowed the maximum advantage to be made of the input current range of the analog-to-digital converter (Data Translation DT2834/5712 8-channel/12-bit). An Apple IIe microcomputer, running the Applesoft Basic software written by Gentle,[1] was used to measure and display the signal.

As the Fluke 410B power supply was monopolar, a floating power supply of 40 V was required to provide the true baseline so that all fluctuations due to noise and integrator overshoot were recorded. Any phase change in the signal could then be corrected by either repositioning the analyzer to the opposite side of the null position, or by reversing the polarity of the bias voltage. The response time of the integrated signal was then controlled, through adjustment of the analyzer offset and the sensitivity of the lock-in amplifier, to optimise the loop gain.

2.3 MODIFICATIONS TO THE APPARATUS

2.3.1 Gas Kerr Cell

The original Kerr cell consisted of nickel-plated steel bar electrodes housed in a brass pressure vessel capable of operating up to 1000 kPa and 500 K. Kerr-effect measurements by previous researchers[1,5,6] on a number of relatively reactive species brought about deterioration in the condition of this cell. A new gas Kerr cell was, therefore, constructed to carry out all measurements reported in this thesis.

The dimensions of the new cell were exactly the same as the original version, described by Gentle.[1] The scope of compounds to be investigated was similar to those previously considered, and so the operational ranges of room temperature to 500 K and vacuum to 1000 kPa pressure were retained. This maximum temperature is a reasonable practical limit because laser-beam bending, due to inhomogenous gas density and the

inverse relationship between the Kerr constant and temperature, made measurements at higher temperatures extremely difficult and of questionable value. As the majority of species investigated had low volatilities, no attempt was made to adapt the gas Kerr cell to operate below room temperature

Due to the deterioration of the brass pressure vessel of the original cell, the replacement vessel was constructed from stainless steel. The end and electrical feed-through flanges were tig-welded to the main cylinder, whereas in the brass cell they were silver soldered. This steel pressure vessel was, therefore, designed to operate under the same physical conditions as the brass version, but with a greatly enhanced resistance to chemical corrosion. Even with this new arrangement, it was noted during the course of these studies that the reactivity of many of these compounds, combined with the presence of reasonably large voltages and the low level of efficiency of the vacuum system, resulted in a build-up of chemical residues in the gas Kerr cell. A regime of regular cell disassembly and cleaning was practised to facilitate the long term operation of the apparatus and to prevent contamination of the sample vapour. It is expected that a continuation of this procedure, though time consuming and demanding, will be rewarded by an extension of the lifetime of this equipment.

The electrical feedthroughs consisted of spring-loaded heads, with rounded surfaces, which were threaded on to connecting rods (all constructed of stainless steel). These were connected by shielded copper cables to the power supplies. The upper electrode was arbitrarily attached to the dc power supply and the bottom electrode to the ac power supply, with the connections being held by the spring-loaded heads. Macor ceramic blocks, bolted to the flanges and sealed using O-rings, insulated the feedthrough rods from the body of the pressure vessel. The surfaces of the insulators were rounded and glazed to prevent tracking. Both the feedthroughs and the insulators were machined to previous designs[1] at the same time as the new gas Kerr cell.

The window mounts were the originals used by Gentle and were made of brass. These were retained as the O-rings form a seal with the windows themselves and the mounts should not come into contact with the sample vapour. The windows used were

generally the Schott BK7 optical flats described by Gentle.[1] Circumstances dictated their periodic cleaning and a second set of windows was occasionally used. These were 13 mm diameter, 9.5 mm thickness, $\lambda/10$ wedged fused silica (Ealing Electro-Optics), which had a static retardance of $< 10^{-2}$ rad. Good mechanical and thermal stability were exhibited by the fused silica windows and no degradation in the accuracy of the measurements was observed with their use. The window mounts were similar to those used for the BK7 windows.

As with the original brass Kerr cell, heating and insulation were provided by grounded electrical heating tape with successive layers of Refrasil insulation cloth, Kaowool ceramic fibre and fibreglass lagging around the body of the cell. Ceramic blocks were used to insulate the ends of the cell and the optical rail. A West Opus 70 microprocessor temperature controller, in conjunction with a J-type thermocouple and a 500 K thermal fuse, maintained set temperatures to $\pm$ 0.3 K for an indefinite period.

2.3.2 Electrodes

The electrode assembly was identical to that used by Gentle.[1] It consisted of a pair of 0.500 m long by 2.5 cm square bars, securely mounted by three pairs of Macor glass-ceramic insulating supports. A Rogowski-type end profile[7] ensured that the integral of the square of the electric-field strength over the pathlength of the field could be accurately determined. The electrode separation (approximately 5 mm) was measured using a ball gauge and micrometer, at up to a dozen evenly spaced positions, to a resolution of 0.1%. The maximum deviation from the mean separation was found to be less than 0.4%. This separation was routinely checked and remeasured throughout the course of this work.

Most of the Kerr-effect measurements undertaken in this work involved the "measurement electrodes", constructed of nickel-plated SC23 high temperature steel, as described by Gentle.[1] These electrodes demonstrated a remarkably low degree of distortion and their mean separation remained effectively unchanged over the temperature

range used. Concern over the consistency and reliability of the plating process, and a desire to extend the range of species able to be investigated, resulted in a second set of electrodes being built to the same dimensions as the first. The new electrodes were made from Hastelloy C-22 (Sandvik Pty Ltd), as this alloy provided the highest degree of chemical and corrosion resistance commercially available. Therefore, no plating was required. Unfortunately, difficulties in the machining process induced stress into the electrodes, which could not be relieved. At temperatures above 390 K, hysteresis led to distortion of the electric field and the new electrodes were only successfully used for the low temperature measurements on bromomethane.

2.3.3 Gas- and Vapour-Handling System

A simplified version of the vapour-handling system described by Gentle[1] was used, and is shown in Figure 2.3 This was constructed from stainless steel tubing joined by Swagelok fittings. The whole assembly was supported by a steel frame. Whitey trunnion-type ball valves and Nupro bellows valves were used. Electrical heating tape and fibreglass lagging provided heating up to 420 K for all shaded piping in Figure 2.3. The first pressure transducer, always open to the vapour-handling system, was an MKS Baratron 221A-10000A model (1300 kPa maximum calibrated pressure), while the MKS Baratron 221A-01000A transducer (130 kPa maximum calibrated pressure) could be sealed off from the system, and was used for less volatile species. Both had an accuracy of 0.5%, were attached by means of Cajon Ultra-Torr connectors and could be thermostated to 380 K by a temperature-controlled heating bulb and fibreglass insulated housing.

The sample gas was evacuated through liquid nitrogen traps by an Alcatel 2008A vacuum pump. The system at vacuum generally leaked less than 150 Pa per hr. A carbon dioxide cylinder was attached for system accuracy checks. Various fittings could be interchanged by a gasket to allow the safe handling of gas lecture bottles, or 50 cm^3 stainless steel flasks for holding liquids and solids. These could be heated by a

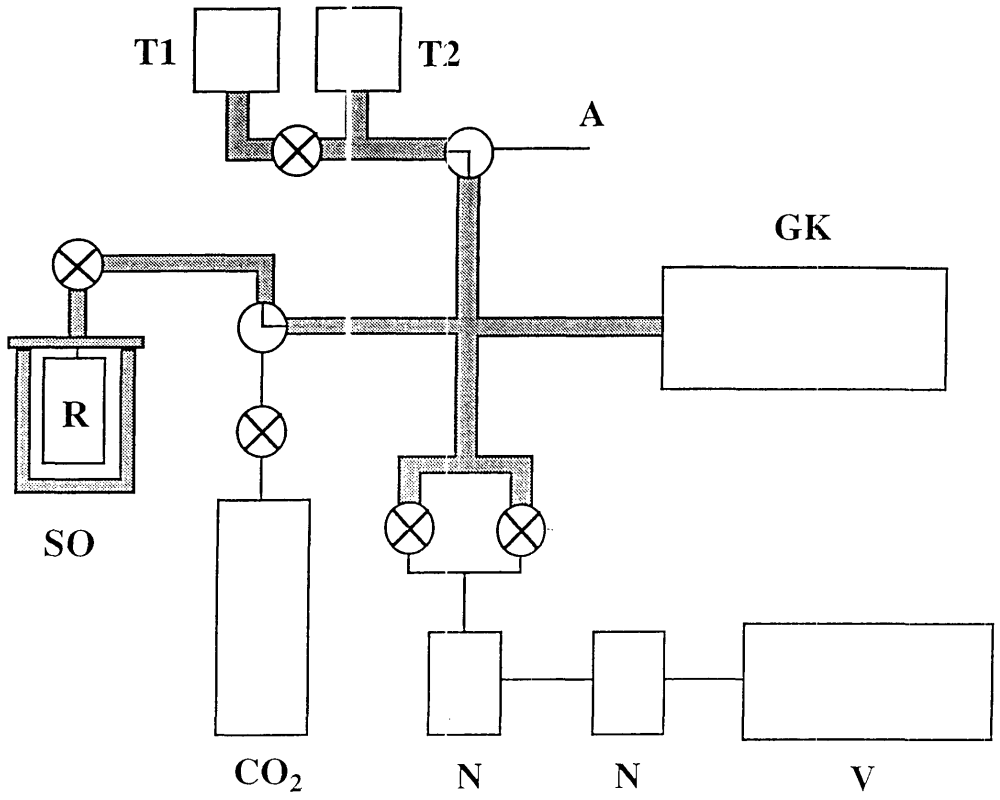

Figure 2.3 Gas- and vapour-handling system for the Kerr-effect apparatus.

T1; 0-130 kPa pressure transducer; **T2**, 0-1300 kPa pressure transducer; **A**, air bleed; **GK**, gas Kerr cell; **R**, sample reservoir; **SO**, sample oven; **CO_2**, carbon dioxide cylinder; **N**, liquid nitrogen trap; **V** vacuum pump

temperature controlled thermos-type oven.

2.3.4 The Laser and Detector

Over half of the compounds were investigated with the 2 mW LE202CP He-Ne laser and photomultiplier tube inherited from previous workers.[1,5,6] The photomultiplier, housing and laser-line filter have been described by Vrbancich.[2] These were replaced by a higher power He-Ne laser and a silicon photodiode for the work on

the bromomethanes, methylacetylenes and fluoroethane. The Spectra-Physics model 106-1 laser was rated at > 10 mW at 632.8 nm in the TEM_{00} mode and exhibited 0.5% rms maximum noise and a 1.2 mrad beam divergence. The low-noise silicon photodiode had an effective area of 7.5 mm^2 and operated in the photovoltaic mode. This type of photodiode is known to possess a quantum efficiency much higher than that of photomultiplier tubes, at a wavelength of 632.8 nm.[8] The detected signal was boosted by a high-accuracy, high-gain FET amplifier. The problems of photodiode insensitivity and mechanical instability noted by Gentle[1] were not observed. The background noise level for this new arrangement was approximately 20% that of the original version of the detection system.

2.4 THE PRINCIPLE OF THE EXPERIMENT

In the limit of low density, the measured Kerr constant, ${}_mK_0$, is related to the Kerr first and second virial coefficients by the equation[9,10]

$$ {}_mK_0 = A_K + \left[B_K + A_K\left(2A_\varepsilon + \tfrac{1}{2}A_r\right)\right]V_m^{-1} \qquad (2.1) $$

where A_ε is the low-density molar dielectric polarization, which is related to the mean static polarizability by

$$ A_\varepsilon = \left(N_A/3\varepsilon_0\right)\left[\alpha^0 + \left(\mu^2/3kT\right)\right] \qquad (2.2) $$

and A_r is the molar refractivity. The low-density Kerr constant is obtained from an indirect measurement of the induced birefringence. As linearly polarized light traverses the electric field, a phase difference between the electric vector components parallel and perpendicular to the field direction is produced. The resultant degree of ellipticity is characterized by the phase angle, or retardance, φ, which is related to the birefringence by

$$\varphi = (2\pi l/\lambda)(n_{\parallel} - n_{\perp}) \tag{2.3}$$

where l is the field pathlength and λ is the vacuum wavelength of the light. As the birefringence is dependent upon the strength of the applied field, the retardance may also be related to the experimental conditions through

$$\varphi = k_1(V_1 + V_0 \sin \omega t)^2 \tag{2.4}$$

in which k_1 is a constant for the gas Kerr cell dependent upon the composition, temperature and pressure of the gas sample, V_1 is the applied dc voltage and $V_0 \sin \omega t$ is the ac voltage, as shown in Figure 2.4. The ellipticity is converted to a rotation by the quarterwave plate and is detected by the analyzer. The lock-in amplifier detects the modulated fundamental frequency and the feedback system then applies a dc voltage, V_2, to the reference Kerr cell. This induces a retardance in the reference Kerr cell, which nulls the retardance produced in the gas Kerr cell, regardless of the size of the bias voltage. Maintenance of the null by the feedback loop then allows for automated sampling with long averaging periods.

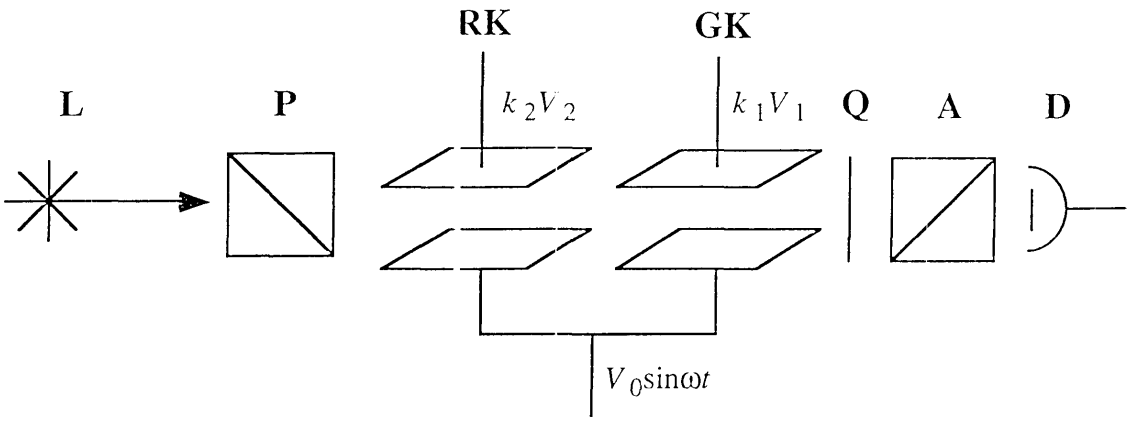

Retardance		φ_2	φ_1	$\frac{\pi}{2}$	
Azimuth	$\frac{\pi}{4}$	0	0	$\frac{\pi}{4}$	$-\frac{\pi}{4} - \theta_0$

Figure 2.4 Optical configuration of the Kerr-effect experiment.

The nulling condition may be examined algebraically by means of Mueller calculus.[11,12] The light beam is represented by the Stokes vector $\{I, M, C, S\}$, with the four parameters representing the intensity, horizontal linear preference, $+45°$ linear preference and the right circular preference, respectively.

All optical components in Figure 2.4 are labelled as for Figure 2.1. The position of the azimuth is determined with respect to the horizontal axis, parallel to the plane of the electrodes. Optical components are represented by 4×4 real matrices. The polarizer and analyzer are treated as ideal homogenous linear polarizers, represented by

$$\frac{1}{2}\begin{bmatrix} 1 & \cos 2\alpha & \sin 2\alpha & 0 \\ \cos 2\alpha & \cos^2 2\alpha & \cos 2\alpha \sin 2\alpha & 0 \\ \sin 2\alpha & \cos 2\alpha \sin 2\alpha & \sin^2 2\alpha & 0 \\ 0 & 0 & 0 & 0 \end{bmatrix}$$

where α is the azimuth of the transmission axis. The two Kerr cells are treated as ideal homogenous linear retarders with a fixed azimuth and relative retardance given by equation 2.4, while the quarterwave plate is an ideal homogenous linear retarder with a relative retardance of $\pi/2$. An ideal homogenous linear retarder is represented by the Mueller matrix

$$\begin{bmatrix} 1 & 0 & 0 & 0 \\ 0 & \cos^2 2\rho(1-\cos\varphi)+\cos\varphi & \cos 2\rho \sin 2\rho(1-\cos\varphi) & -\sin 2\rho \sin\varphi \\ 0 & \cos 2\rho \sin 2\rho(1-\cos\varphi) & 1-\cos^2 2\rho(1-\cos\varphi) & \cos 2\rho \sin\varphi \\ 0 & \sin 2\rho \sin\varphi & -\cos 2\rho \sin\varphi & \cos\varphi \end{bmatrix}$$

in which ρ is the azimuth of the fast axis. Analysis of the optical train proceeds by the multiplication of the Stokes vector with each matrix in turn, and only the intensity of the light modulated at the frequency ω is detected. This is found to be

$$2I_\omega = (k_1V_1 + k_2V_2)\left\{2k_1V_1^2 + 2k_2V_2^2 + V_0^2(k_1 + k_2) + 4\theta_0\right\}V_0 \sin\omega t \qquad (2.5)$$

which gives a null condition of

$$k_1 V_1 = -k_2 V_2. \tag{2.6}$$

Thus, the null condition is independent of the ac voltage and the offset of the azimuth of the analyzer, θ_0. The magnitude of the analyzer offset and the ac voltage do, however, affect the sensitivity of the experiment and the uncertainties.

2.5 ERROR ANALYSIS AND ALIGNMENT PROCEDURE

An error analysis for the optical components of the Kerr-effect experiment has previously been performed by Gentle,[1] using Mueller calculus. It was established that a misalignment of the gas Kerr cell of 1° results in an error in the observed cell constant of less than 0.06%. An accurate spirit level was used to align the gas Kerr cell. As the reference Kerr cell was calibrated in position, any small misalignment would not affect its calibration constant. A static retardance in any of the windows of the two Kerr cells may give rise to an error in the null.[13] For azimuths of 0° or 90°, no errors in the null condition occur, although, for an azimuth of 45°, a stray retardance of 5×10^{-2} rad leads to an error of 0.15%. The windows used have retardances much smaller than this.

The orientation of the transmission axis of the polarizer was established using a polarizing microscope. As necessary, the analyzer was nulled photometrically using the nulled polarizer, lock-in amplifier and a Faraday-coil modulator. An identical procedure was used to null the quarterwave plate. The micrometers used to orientate each of these components allowed the azimuths to be set to within 10^{-5} rad. An error of this size in the orientation of the quarterwave plate had no effect on the null condition.

There were, of course, several other sources of error in the experiment. These included the reference Kerr cell and bias power supply calibrations, already discussed, and the pressure and temperature measurements. The overall absolute uncertainty of the measured Kerr constants is estimated at ± 3%. This uncertainty is larger than the ± 2%

previously cited for this apparatus [14] with the decrease in the absolute level of precision arising from the bias power supply recalibration. However, the repeatability of both this calibration and the Kerr-effect measurements were significantly better than this.

A general estimation of the accuracy of the experiment and the measured Kerr constants was also obtained through routine measurements on carbon dioxide. The Kerr effect of this species has been measured using the original version of this apparatus[1] with a high level of precision and accuracy. These previous results were used as a basis of comparison for the more recent measurements on carbon dioxide. Such accuracy checks were routinely performed before, throughout and after each of the investigations reported in the following chapters. Agreement was usually within 1% and a deviation of greater than 1.5% led to the immediate cessation of the measurements and a search for, and elimination of, the error. As several of the compounds investigated were to some extent reactive in the gas Kerr cell, due to reasons already mentioned, this usually involved the dismantling and cleaning of the cell, including the pressure vessel, the electrode assembly, the end windows and the electrical feedthroughs. Regardless of the source of error, no further measurements were attempted until the carbon dioxide readings were again repeatedly shown to be within at least 1% agreement with the previous results at several temperatures.

This method had also been used successfully by Gentle[1] to detect long-term changes in the electrode spacings, orientation of the optical components and the computer analog input module. Although these factors did contribute to a slow drift in the calibration, the main source of any error in the carbon dioxide 'accuracy checks' was the presence of decomposition residues of the investigated compounds in the gas Kerr cell. It should also be emphasised that the results of the accuracy checks on carbon dioxide were not used in any way to scale the experimental results for the sample gas or vapour.

2.6 MEASUREMENT PROCEDURE

After the carbon dioxide accuracy checks were satisfactorily performed, the gas Kerr cell was evacuated for ≈ 30 min. The sample vapour was used first to flush the system, and then the gas Kerr cell was filled to a maximum of two-thirds of the equilibrium vapour pressure at the particular temperature. The temperature and pressure of the vapour were allowed to equilibrate for 0.5 - 1.0 hr before the commencement of measurements. These consisted of recording the nulling voltages applied to the reference Kerr cell for successive cycles of gas Kerr-cell bias voltage off / voltage on, with the latter two-thirds of each being averaged. This procedure gave an accurate measure of the induced birefringence and removed both any drift and the influence of extraneous light over the course of the measurements. The sampling time was entered through the software and varied from 16 - 100 minutes, depending upon the magnitude of the birefringence observed. The nulling voltages were automatically averaged by the software and printed, together with the standard deviation and the vapour pressure.

A portion of the vapour sample was then evacuated and the remainder allowed to equilibrate for 5 - 40 min at the new pressure before recommencing measurements. All measurements at each temperature were completed in the course of a day, as it was considered undesirable to leave the sample vapour in the Kerr cell for longer periods. After the last measurement, the cell was evacuated for ≈ 30 min and allowed to equilibrate at a new temperature.

The sample pressure of the vapour was recorded from either of the two pressure transducers, which were calibrated against the atmospheric pressure. This was measured daily using a mercury manometer (A.L. Franklin) accurate to ± 7 Pa. As explained by Gentle,[1] the effective temperature was determined by means of a thermocouple, placed inside a probe tube built into the pressure vessel.

The molar Kerr constant can be expressed, from equations 1.1 and 2.3, in terms of the experimental observables as

$$ {}_{m}K_0 = \left(\lambda d^2 V_m / 27\pi l\right)(k_2 V_2 / V_1). \qquad (2.6) $$

Measured values of ${}_{m}K_0$ were then graphed against V_m^{-1} for each pressure to yield A_K and B_K at a particular temperature. The errors quoted for A_K and B_K were determined from the statistical uncertainties generated in fitting the values of ${}_{m}K_0$ to the density data. This fitting generally proceeded by weighting the measured Kerr constant to the inverse square of its standard deviation. For those density dependence studies where one, or a few, of the measured Kerr constants had very small standard deviations compared to the majority of Kerr constants measured at that temperature, a similar procedure was used. These very small statistical deviations, randomly produced as a consequence of large nulling voltages, were occasionally found to bias the fit to the data when the inverse square of the standard deviation fitting technique was used. Whenever this was judged to have occurred, the data were fitted without weighting the points.

Examples showing pressure dependences analyzed by the two techniques are given in Figures 2.5 and 2.6. In Figure 2.5, the density dependence was analyzed using a weighting factor of the inverse square of the standard deviation of each point. The Kerr constants at the lowest three gas densities have larger uncertainties as the background noise of the experiment is approximately independent of the magnitude of the birefringence. In Figure 2.6, the unbroken line represents the unweighted fit to the data, which was used in the analysis for the Kerr virial coefficients of dibromomethane at this temperature. The dashed line corresponds to the inverse square of the standard deviation fit. This was not used, as the Kerr constants at the three highest densities unduly bias this method, giving rise to a gradient which is too steep and would result in an A_K value 2% larger than that produced by the unweighted fit.

The temperature dependence of A_K was then used to determine the electric properties of the molecule of interest. The uncertainties quoted for these properties were calculated from a standard propagation of errors technique at the one-standard deviation level.

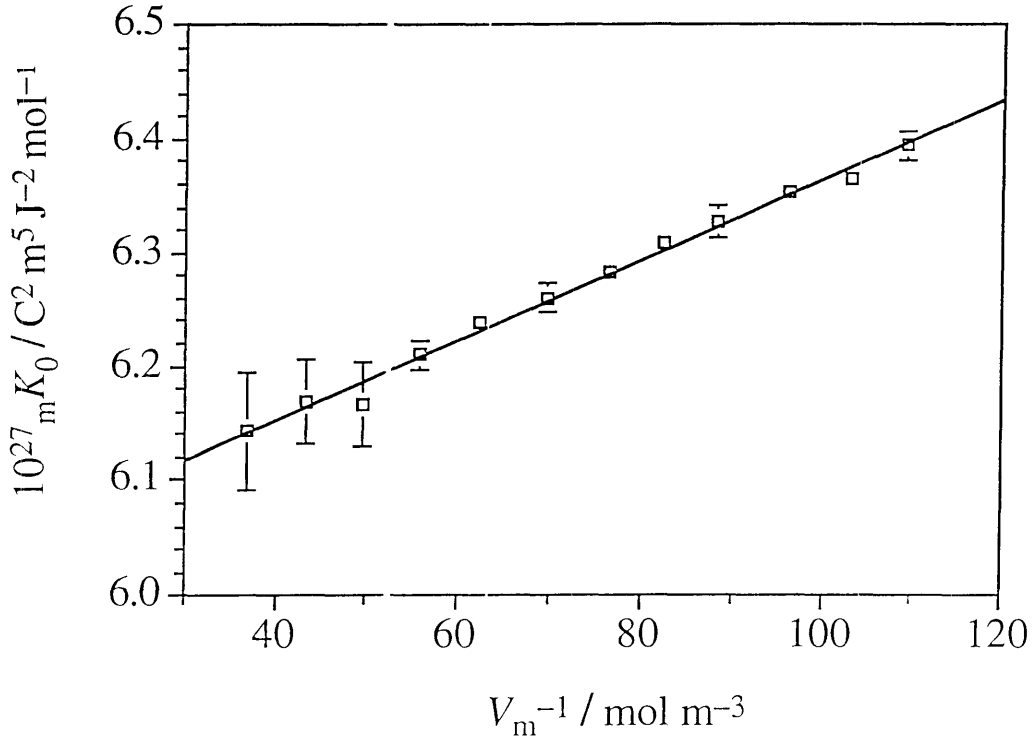

Figure 2.5 Density dependence of the Kerr effect of ammonia at 297.5 K.

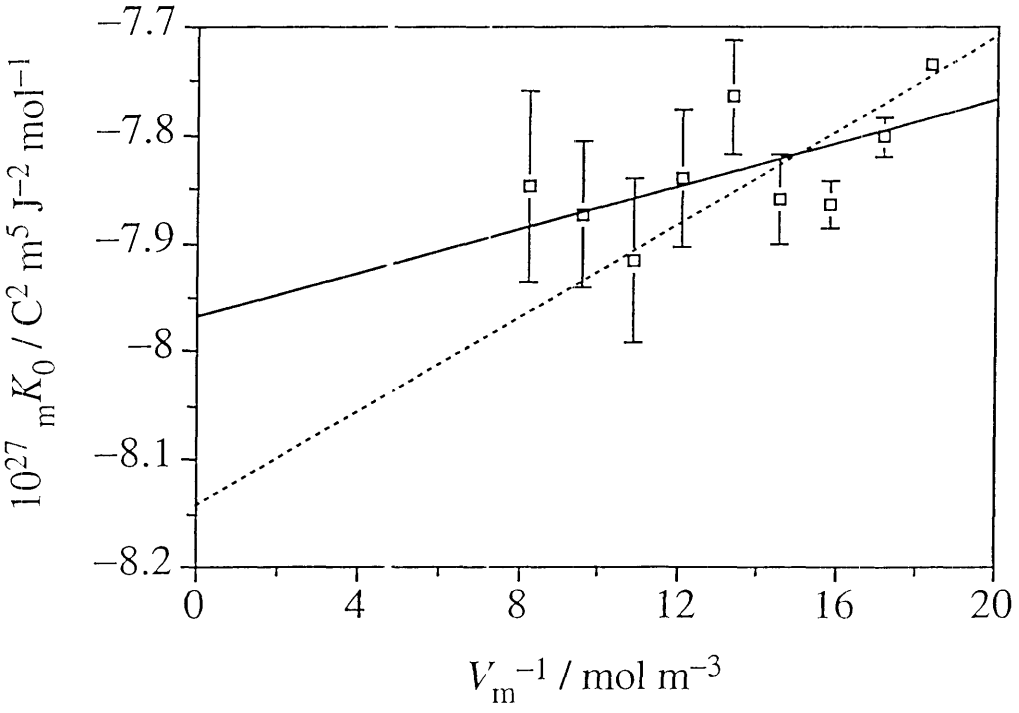

Figure 2.6 Density dependence of the Kerr effect of dibromomethane at 454.2 K.

2.7 RAYLEIGH LIGHT-SCATTERING APPARATUS

Several of the Rayleigh light-scattering results for the fluorobenzenes, reported in Chapter 6, were measured by the author. The configuration of the apparatus is depicted in Figure 2.7 and a brief description follows. This is identical to the apparatus constructed by Hesling[15] and designated version two.

Radiation at 632.8 nm from a 10 mW He-Ne laser (Spectra Physics 106-1) was orientated with the plane of polarization set to the vertical. A Glan-Taylor polarizing prism ensured that only vertically polarized light was transmitted. Several stops were used to reduce divergence of the beam and to minimise extraneous light. After passing through a light chopper, the beam entered the scattering cell through Brewster angle

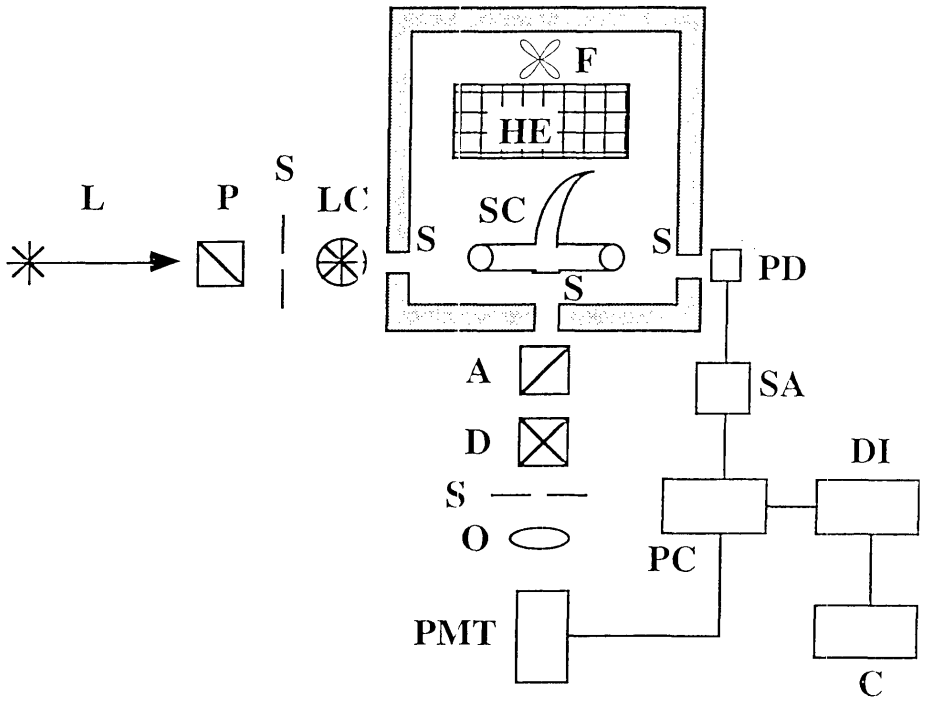

Figure 2.7 Rayleigh light-scattering apparatus.

L, laser; **P**, polarizer; **LC**, light chopper; **S**, stop; **SC**, scattering cell; **HE**, heating element; **F**, fan; **A**, analyzer; **D**, depolarizer; **O**, optical lens; **PMT**, photomultiplier tube; **PD**, photodiode; **SA**, signal amplifier; **PC**, photon counter; **DI**, digital interface; **C**, microcomputer

windows (Francis Lord B270 glass), attached to the sidearms of the scattering cell by an inert resin (Torr Seal). The scattering cell was constructed from silica and featured a scattering window oriented at 90° to the direction of the beam. A large Wood's horn opposite this, and smaller versions under each of the Brewster angle windows, trapped internally scattered and refracted light. Unscattered light passed through the rear Brewster angle window and was incident upon a photodiode.

Perpendicularly scattered light passed through the scattering window and an analyzer, which could be accurately positioned to select either vertically or horizontally polarized light. A depolarizer was attached to the same rotatable mount as the analyzer to remove the problems of polarization-dependent absorption by other optical components and polarization-dependent sensitivity of the photomultiplier. An interference filter (632.8 nm with a half-height band width of 12.1 nm) could be mounted with the depolarizer to remove vibrational Raman lines. This was not required for the molecules measured by the author, because the vibrational contributions were expected to be small for such anisotropic species.[16,17] The perpendicularly scattered light was detected by a photomultiplier tube (RCA model C31034A), housed in a refrigerated chamber at 253 K, after traversing a pair of vacuum sealed windows.

The signal from the photomultiplier was passed through a preamplifier (ORTEC/Brookdeal Model 9301) to the photon counter (ORTEC/Brookdeal Model 5C1 dual channel). A photodiode in the path of the chopped, unscattered light sent a gating signal to the photon counter. This initiated separate counters to synchronously record the signal pulses for the "on" and "off" periods of the laser. The background signal could, therefore, be subtracted from the observed signal on a continuous basis.

All optical components, except the scattering cell, were mounted by magnetic blocks or optical stands to a steel frame. This was supported by thick rubber bases to dampen external vibrations. The scattering cell was securely clamped to the optical frame. Both the polarizer and the analyzer were mounted in rotatable holders, which allowed their precise alignment.

In order to minimise extraneous light, the interior of the oven, exterior of the

scattering cell and the magnetic blocks were painted matt black and a black-painted box similarly shielded the analyzer, depolarizer and optical lens. Black rubber tubing was used to make light-tight seals between this box and the photomultiplier tube housing and the scattering window and the adjacent stop. All laboratory windows were blacked out.

Figure 2.8 depicts the vapour handling system for the Rayleigh light-scattering apparatus. The scattering cell was housed in a styrofoam-insulated oven with a heating element powered by a Type W20 Variac. A fan provided uniform heating to 360 K. The sample reservoir was attached by a Cajon fitting to stainless steel tubing. This was wrapped in heating tape and glass-fibre insulation. A filter (pore size ≈ 0.05 μm) removed dust from the sample vapour, before it entered the scattering cell through another Cajon fitting. The vapour pressure was measured by a pressure transducer (Data Instruments SA25A).

2.8 RAYLEIGH LIGHT-SCATTERING MEASUREMENTS

For any sample vapour, the procedure for measuring the depolarization ratio was as follows. At one of the two alternative analyzer positions, the intensity of the

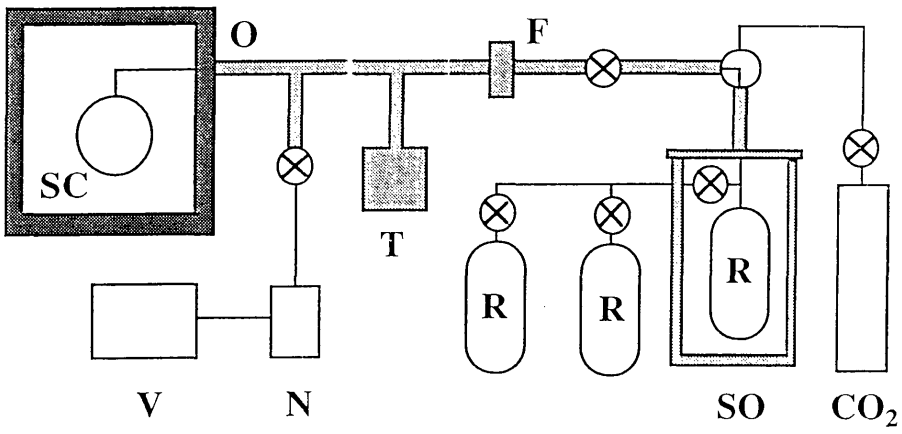

Figure 2.8 Gas- and vapour-handling system for the Rayleigh light-scattering apparatus. **O**, oven; **F**, filter; **SC**, scattering cell; **T**, pressure transducer; **R**, sample reservoir; **V**, vacuum pump; **N**, liquid nitrogen trap; **SO**, sample oven; **CO_2**, carbon dioxide cylinder

spuriously scattered light from the evacuated scattering cell was measured. The scattering cell was then flushed with the sample vapour, filled to less than two-thirds of the equilibrium vapour pressure and the scattering intensity from the sample was measured. Then the analyzer was rotated by 90° to the alternative position and the scattering intensity at the new position, and the same pressure, was measured. This was followed by the evacuation of the sample and measurement of the spurious scattering at the second position. Subtraction of the background light-scattering from the corresponding sample light-scattering gave the depolarization ratio from equation 1.25. This procedure was repeated at different pressures to obtain an averaged depolarization ratio. Experimental uncertainties were determined by standard propagation of errors at the one-standard deviation level.

Before measurement of the depolarization ratio of a sample, the reliability of the apparatus was checked by the measurement of the depolarization ratio of carbon dioxide. Any disagreement with the value determined by Hesling[15] of $100\rho_0 = 4.01 \pm 0.04$ led to the isolation and correction of the fault. Liquid samples were degassed before use.

Mean polarizabilities were determined, using equation 1.27, by measuring the density dependence of the polarized light scattering of the sample and comparing it with that of argon. The mean polarizability of argon was taken from reference 18.

Descriptions of the alignment procedure and error analysis for the Rayleigh light-scattering apparatus have been given by Hesling[15] and will not be repeated here. The total systematic error of the apparatus was $< 0.5\%$.

2.9 DISCUSSION

Systematic studies of the density- and temperature dependence of the Kerr effect in gases were pioneered by Buckingham and coworkers. In the first version of this apparatus,[19] the birefringence in the gas Kerr cell was induced by an ac voltage, which was nulled at 2ω by an ac voltage superimposed on a dc bias in a reference Kerr cell.

Signal amplification was provided by a second, and larger, dc bias being applied to the reference Kerr cell. An improved version of this apparatus was used to carry out further studies on a range of molecules.[9,10,20] Burnham et al.[21] also used a similar design to measure the Kerr effects of substituted methanes.

Buckingham and Sutter[22] used an alternative approach to measure the Kerr effect in a series of alkanes. No modulation was applied to their gas Kerr cell and both the signal modulation and nulling retardation were provided by two independent Faraday coils. More recently, Tammer and Hüttner[23] have used a similar set of apparatus.

A significant improvement has been reported for the apparatus developed by Shelton.[24] In this experiment, the modulated sample signal is generated by applying large ac and dc voltages to the gas Kerr cell, with signal amplification being provided by a large dc bias voltage on the liquid Kerr cell. The intensity of this signal is compared with that produced when the ac voltage is removed from the gas Kerr cell and a smaller modulation is applied to the liquid Kerr cell.

Reported measurements from Tammer et al.'s and Shelton's apparatus have been limited to relatively small and volatile gases.[23,25-28] As already described in this chapter, an improvement has been made in the signal-to-noise ratio for the latest version of this Kerr-effect apparatus, yet it still does not exhibit the nanoradian sensitivity observed with Shelton's apparatus.[29] It is, therefore, evident that further improvements can be made. However, it is unlikely that these improvements would translate fully through to the results of many of the compounds likely to be investigated in the future. This is due to the low volatility and reactivity of such species introducing practical difficulties which would overshadow marginal advances in the detection system. Although further improvements are foreseen in the design of the present apparatus, in light of the experiences gained in performing these measurements, the possibility of obtaining results at the high levels of precision and accuracy claimed for simple molecules is not realistic for larger polyatomic species.

2.10 REFERENCES

1 Gentle, I.R., *Ph.D. Thesis* (University of Sydney, 1987).

2 Vrbancich, J., *Ph.D. Thesis* (University of Sydney, 1979).

3 Vrbancich, J., Bogaard, M P. and Ritchie, G.L.D., *J. Phys. E: Sci. Instrum.*, **14**, 166 (1981).

4 Jessop, H.T., *Brit. J. Appl. Phys.*, 4, 138 (1953).

5 Stankey, R., *M.Sc. Thesis* (University of New England, 1991).

6 Watson, J.N., *B.Sc. Honours Thesis* (University of New England, 1990).

7 Cobine, J.D., *Gaseous Conductors: Theory and Engineering Applications* (Dover Publications, New York, 1958).

8 Shelton, D.P., and Cameron, R.E., *Rev. Sci. Instrum.*, **59**, 430 (1988).

9 Buckingham, A.D. and Dunmur, D.A., *Trans. Faraday Soc.*, **64**, 1776 (1968).

10 Buckingham, A.D. and Orr, B.J., *Proc. Roy. Soc. A*, **305**, 259 (1968).

11 Mueller, H., *J. Opt. Soc. Am.*, **38**, 661 (1948).

12 Shurcliff, W.A., *Polarized Light: Production and Use* (Harvard University Press, Cambridge, Mass., 1962).

13 Buckingham, A.D., and Disch, R.L., *Proc. Roy. Soc. A*, **273**, 275 (1963).

14 Gentle, I.R., Laver, D.R. and Ritchie, G.L.D., *J. Phys. Chem.*, **93**, 3035 (1989).

15 Hesling, M.R., *Ph.D. Thesis* (University of New England, 1991).

16 Bridge, N.J. and Buckingham, A.D., *Proc. Roy. Soc. A*, **295**, 334 (1966).

17 Bogaard, M.P., Buckingham, A.D., Pierens, R.K. and White, A.H., *J. Chem. Soc., Faraday Trans. I*, **74**, 3008 (1978).

18 Landolt-Börnstein, *Zahlenwerte und Funktionen*, Band II, Teil 8 (Springer, Berlin, 1962).

19 Boyle, L.L., Buckingham, A.D., Disch, R.L. and Dunmur, D.A., *J. Chem. Phys.*, **45**, 1318 (1966).

20 Buckingham, A.D., Bogaard, M.P., Dunmur, D.A., Hobbs, C.P. and Orr, B.J., *Trans. Faraday Soc.*, **66**, 1548 (1970).

21 Burnham, A.K., Buxton, L W. and Flygare, W.H., *J. Chem. Phys.*, **67**, 4990 (1977).

22 Buckingham, A.D. and Sutter, H., *J. Chem. Phys.*, **64**, 364 (1976).

23 Tammer, R. and Hüttner, W., *Chem. Phys.*, **146**, 155 (1990).

24 Shelton, D.P., *Rev. Sci. Instrum.*, **64**, 917 (1993).

25 Tammer, R. and Hüttner, W., *Chem. Phys.*, **168**, 151 (1992).

26 Tammer, R. and Hüttner, W., *Mol. Phys.*, **83**, 579 (1994).

27 Shelton, D.P. and Rugar, B., *Chem. Phys. Lett.*, **201**, 364 (1993).

28 Shelton, D.P. and Palubinskas, J.J., *J. Chem. Phys.*, **104**, 2482 (1996).

29 Shelton, D.P. and Cameron, R.E., *Rev. Sci. Instrum.*, **59**, 430 (1988).

CHAPTER 3 - ELECTRIC POLARIZABILITIES AND HYPERPOLARIZABILITIES OF THE METHYLAMINES

3.1 INTRODUCTION

The series of compounds ammonia, methylamine, dimethylamine and trimethylamine provides an excellent opportunity to compare polarizabilities and hyperpolarizabilities determined by a variety of experimental and theoretical techniques. The electric properties of ammonia, in particular, have been of considerable interest. Ammonia is also the only compound in this series to have been investigated previously as a vapour by the Kerr effect, in early measurements by Szivessy[1] and Breazeale.[2]

Solution-phase Kerr-effect studies have also been reported by Aroney et al.[3,4] for ammonia and trimethylamine in a range of solvents. The Kerr constants of these molecules, and the apparent polarizability anisotropy of trimethylamine, were found to be solvent dependent, due to local-field effects. Measurements on the vapours are required to obtain accurate molecular polarizabilities. Bridge and Buckingham[5] determined the polarizabilities of ammonia from Rayleigh light-scattering experiments at a wavelength of 632.8 nm. Stankey[6] has similarly measured the Rayleigh depolarization ratio and mean polarizability of trimethylamine. The free-molecule, or even the solution-phase, polarizabilities are not known for either methylamine or dimethylamine.

The only previous experimental values for the first and second hyperpolarizabilities of ammonia are from a second harmonic generation experiment at a wavelength of 694.3 nm, by Ward and Miller.[7] However, in the recent literature there are reports of several theoretical studies which have reliably modelled the experimental polarizabilities of ammonia. The accuracy of similar calculations of the hyperpolarizabilities is more difficult to gauge, though, due to the absence of experimental values to provide a basis of comparison. There have been no previously reported values of the hyperpolarizabilities of methylamine, dimethylamine or trimethylamine.

The temperature dependences of the Kerr effects of ammonia and the methylamines were, therefore, investigated with the aim of determining the polarizabilities of methylamine and dimethylamine, and the Kerr first and second hyperpolarizabilities of all four species.

3.2 EXPERIMENTAL

The sources and purities, determined by gas chromatography, of the samples used were as follows: ammonia (Matheson, anhydrous grade), > 99.7%; methylamine (Aldrich, ≥ 98%), > 99.5%; dimethylamine (Aldrich, ≥ 99%), > 99.85%; trimethylamine (Matheson, anhydrous grade), > 99.75%. All samples were used without further purification, as the effects of likely impurities were considered to be negligible.

The gas densities for ammonia and methylamine were calculated using published density second virial coefficients.[8] For dimethylamine, the required data were available only over the temperature range 312.4 - 405.2 K.[8] These known values and the dipole moment of dimethylamine were used to determine the parameters in the Stockmayer potential.[9] This was used to estimate the coefficients for the temperature ranges 293 - 303 K and 410 - 500 K. The accuracy of the force constants, ε/k = 1026 K and σ = 0.237 nm, was assessed by using the derived values of these quantities to recalculate the known virial coefficients. Although these were found to overestimate the tabulated values by up to 18% in the worst case, this still resulted in an error of less than 0.8% in any of the gas densities. For trimethylamine, the density second virial coefficients measured by Lambert and Strong[10] only cover the range 311.2 - 374.7 K. The Stockmayer potential could not be used to determine the virial coefficients outside this range, because the resulting reduced second virial coefficient fell outside the tabulated values. The known virial coefficients for trimethylamine were, therefore, fitted to the function

$$\log|B| = m\log T + C \qquad (3.1)$$

where B is the density second virial coefficient at temperature T, and m and C are the gradient and intercept of the resultant linear plot. This method was shown to be adequate over short extrapolations by the high correlation of the fit.

The results are summarized in Tables 3.1, 3.2, 3.3 and 3.4. The range and number of pressures investigated in order to establish each density dependence are given, together with the corresponding density second virial coefficient, B. Kerr first and second virial coefficients were derived from the density dependence performed at each temperature, and are also listed.

3.3 DISCUSSION

For molecules with a permanent electric dipole moment, the Kerr first virial coefficient is related to the electric properties by

$$A_K = (N_A/81\varepsilon_0)\Big\{\gamma^K + (kT)^{-1}\Big[(2/3)\mu\beta^K + (3/10)\Big(\alpha_{\alpha\beta}\alpha^0{}_{\alpha\beta} - 3\alpha\alpha^0\Big)\Big] + (3/10)(kT)^{-2}\mu^2(\alpha_{zz} - \alpha)\Big\}. \qquad (3.2)$$

The temperature dependences of the Kerr effects of ammonia, methylamine, dimethylamine and trimethylamine are shown in Figure 3.1. The positive Kerr constants and curvature for ammonia provide a marked contrast with those of trimethylamine, although the two molecules have the same symmetry. This will be discussed later in terms of the importance of the various contributions to A_K for these species.

Szivessy[1] measured ${}_mK = 6.56\times10^{-27}$ C^2 m^5 J^{-2} mol^{-1} for ammonia at 589 nm, 101 kPa and 291 K. This is in good agreement with the value of $A_K = 6.30\times10^{-27}$ C^2 m^5 J^{-2} mol^{-1} obtained from this work at 291 K and the longer wavelength of 632.8 nm. The ${}_mK$ values measured by Breazeale[2] for ammonia at 650 nm were generally within 1 % of the results from this work, but as the older measurements were

Table 3.1 Kerr effect of ammonia at 632.8 nm

T / K	Number of Pressures	Pressure Range / kPa	$10^6 B$ a) / $m^3\ mol^{-1}$	$10^{27} A_K$ / $C^2\ m^5\ J^{-2}\ mol^{-1}$	$10^{30} B_K$ b) / $C^2\ m^8\ J^{-2}\ mol^{-2}$
297.5	12	91 - 262	−275	6.030 ± 0.008	2.68 ± 0.09
306.8	12	100 - 319	−246	5.639 ± 0.004	2.73 ± 0.04
319.3	13	109 - 307	−216	5.154 ± 0.008	2.67 ± 0.09
330.2	13	96 - 346	−198	4.845 ± 0.007	2.17 ± 0.07
342.9	11	101 - 322	−182	4.467 ± 0.005	1.99 ± 0.05
356.6	14	124 - 373	−165	4.109 ± 0.009	1.87 ± 0.09
375.7	12	133 - 374	−145	3.686 ± 0.013	1.89 ± 0.13
395.8	12	113 - 335	−127	3.250 ± 0.020	1.86 ± 0.23
422.1	11	137 - 379	−109	2.794 ± 0.031	1.80 ± 0.35
449.9	10	142 - 363	−93	2.541 ± 0.006	1.19 ± 0.07
476.6	12	140 - 404	−83	2.213 ± 0.013	1.32 ± 0.15
483.5	6	102 - 153	−77	2.21 ± 0.09	–
492.1	11	159 - 408	−70	2.124 ± 0.018	0.66 ± 0.21

a) Density second virial coefficients from reference 8. b) Calculated using $10^{40} \alpha / C^2\ m^2\ J^{-1} = 2.47 \pm 0.02$, from reference 5, $10^{40} \alpha^0 / C^2\ m^2\ J^{-1} = 2.60 \pm 0.08$, from reference 11, and $10^{30} \mu / C\ m = 4.90984 \pm 0.00024$, from reference 12.

Table 3.2 Kerr effect of methylamine at 632.8 nm

T / K	Number of Pressures	Pressure Range / kPa	$10^6 B$ a) / $m^3\ mol^{-1}$	$10^{27} A_K$ / $C^2\ m^5\ J^{-2}\ mol^{-1}$	$10^{30} B_K$ b) / $C^2\ m^8\ J^{-2}\ mol^{-2}$
297.3	9	80 - 254	−466	−3.300 ± 0.013	8.4 ± 0.2
305.4	11	66 - 258	−431	−3.120 ± 0.010	7.5 ± 0.1
312.9	10	76 - 196	−403	−3.063 ± 0.008	8.1 ± 0.1
331.8	11	80 - 214	−344	−2.601 ± 0.019	5.9 ± 0.3
348.9	10	86 - 204	−306	−2.372 ± 0.014	4.6 ± 0.2
364.2	12	91 - 212	−274	−2.064 ± 0.011	3.0 ± 0.2
387.0	9	93 - 259	−241	−1.857 ± 0.010	2.8 ± 0.2
411.8	7	90 - 146	−209	−1.467 ± 0.041	−0.9 ± 1.0
451.8	9	101 - 220	−174	−1.265 ± 0.033	1.7 ± 0.7
490.5	9	122 - 215	−147	−0.875 ± 0.023	−1.0 ± 0.5

a) Density second virial coefficients from reference 8. b) Calculated using $10^{40}\alpha\ /\ C^2\ m^2\ J^{-1} = 4.53 \pm 0.05$, from reference 6, $10^{40}\alpha^0\ /\ C^2\ m^2\ J^{-1} = 4.68 \pm 0.14$, from reference 11, and $10^{30}\mu\ /\ C\,m = 4.42 \pm 0.05$, from reference 13.

Table 3.3 Kerr effect of dimethylamine at 632.8 nm

T / K	Number of Pressures	Pressure Range / kPa	$10^6 B$ a) / $m^3\ mol^{-1}$	$10^{27} A_K$ / $C^2\ m^5\ J^{-2}\ mol^{-1}$	$10^{30} B_K$ b) / $C^2\ m^8\ J^{-2}\ mol^{-2}$
294.4	11	36 - 109	−717	−7.889 ± 0.012	14.4 ± 0.4
305.2	12	41 - 118	−643	−7.224 ± 0.021	10.6 ± 0.5
312.6	12	47 - 161	−595	−6.870 ± 0.010	8.9 ± 0.2
328.4	13	43 - 140	−524	−6.173 ± 0.013	6.8 ± 0.3
342.3	13	49 - 150	−478	−5.737 ± 0.017	6.8 ± 0.4
353.2	10	49 - 158	−450	−5.304 ± 0.010	6.3 ± 0.2
364.0	12	60 - 170	−406	−5.039 ± 0.016	5.4 ± 0.3
373.3	9	66 - 166	−391	−4.630 ± 0.010	4.0 ± 0.2
407.5	10	60 - 176	−303	−3.916 ± 0.034	4.8 ± 0.7
439.0	10	54 - 175	−252	−3.194 ± 0.024	3.3 ± 0.6
466.5	9	77 - 175	−216	−2.867 ± 0.024	2.3 ± 0.6
498.7	11	74 - 182	−186	−2.274 ± 0.031	−0.6 ± 0.9

a) Density second virial coefficients from reference 8 and calculated values (see text). b) Calculated using $10^{40} \alpha / C^2\ m^2\ J^{-1} = 6.60 \pm 0.07$, from reference 6, $10^{40} \alpha^0 / C^2\ m^2\ J^{-1} = 6.62 \pm 0.20$, from reference 11, and $10^{30} \mu / C\ m = 3.369 \pm 0.034$, from reference 14.

Table 3.4 Kerr effect of trimethylamine at 632.8 nm

T / K	Number of Pressures	Pressure Range / kPa	$10^6 B$ [a] / $m^3\ mol^{-1}$	$10^{27} A_K$ / $C^2\ m^5\ J^{-2}\ mol^{-1}$	$10^{30} B_K$ [b] / $C^2\ m^8\ J^{-2}\ mol^{-2}$
295.3	11	40 - 110	−756	−4.677 ± 0.021	10.3 ± 0.5
308.0	9	42 - 121	−689	−4.101 ± 0.041	5.4 ± 1.1
312.1	13	40 - 127	−666	−4.099 ± 0.020	7.4 ± 0.5
326.0	12	41 - 127	−599	−3.819 ± 0.015	7.5 ± 0.4
347.3	11	46 - 127	−520	−3.279 ± 0.011	4.7 ± 0.3
367.6	11	48 - 131	−457	−3.067 ± 0.020	7.1 ± 0.5
386.8	13	66 - 190	−395	−2.631 ± 0.019	4.7 ± 0.4
405.3	11	57 - 128	−366	−2.429 ± 0.034	4.4 ± 1.0
427.0	9	62 - 123	−324	−2.108 ± 0.047	4.3 ± 1.6
446.6	8	80 - 175	−293	−1.787 ± 0.012	1.5 ± 0.3
469.8	8	74 - 139	−260	−1.722 ± 0.045	6.9 ± 1.4
490.4	8	65 - 127	−237	−1.406 ± 0.024	2.2 ± 0.9

a) Density second virial coefficients from reference 10 and estimated values (see text). b) Calculated using $10^{40}\,\alpha / C^2\,m^2\,J^{-1} = 8.69 \pm 0.09$, from reference 6, $10^{40}\,\alpha^0 / C^2\,m^2\,J^{-1} = 8.82 \pm 0.26$, from reference 11, and $10^{30}\,\mu / C\,m = 2.041 \pm 0.034$, from reference 15.

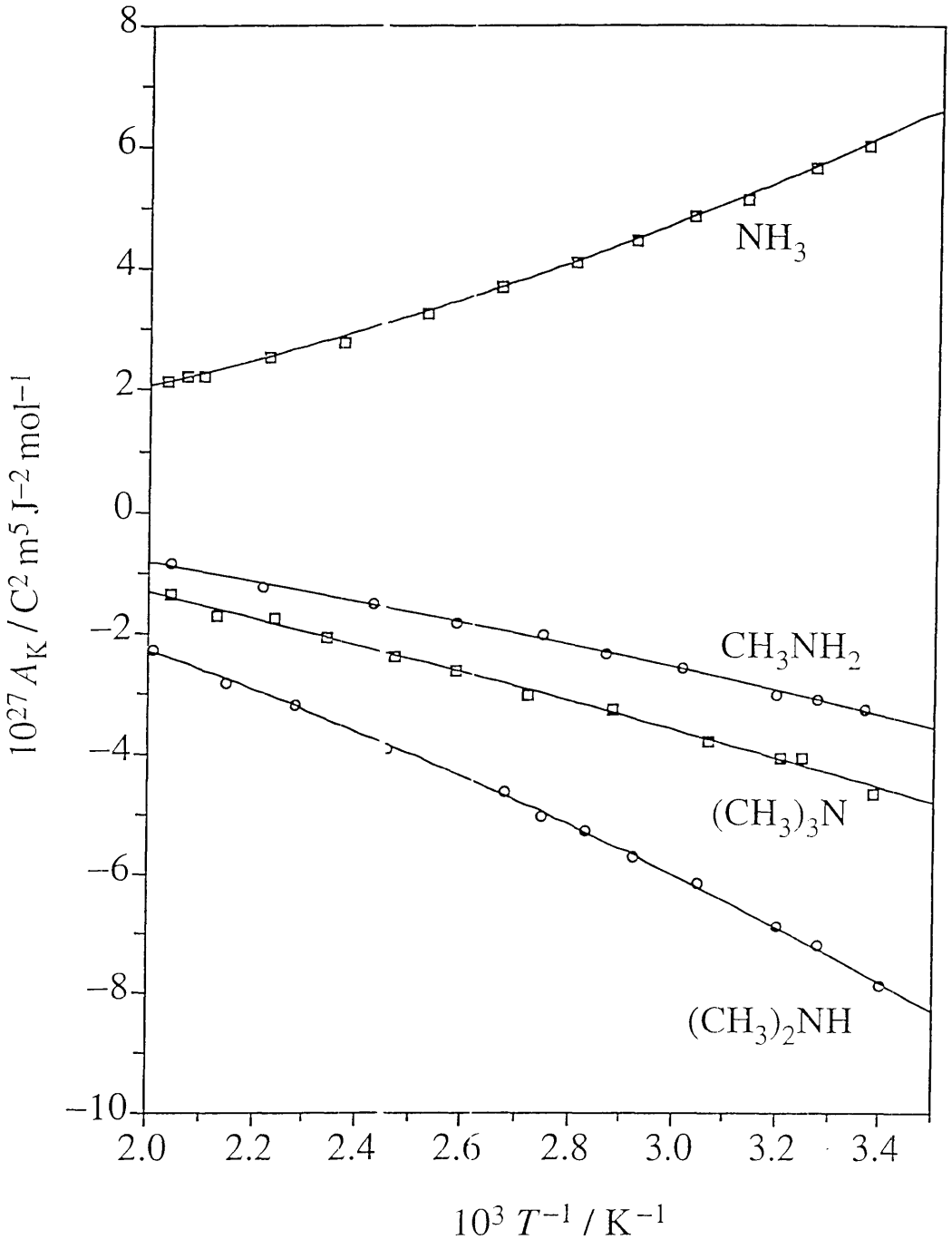

Figure 3.1 The temperature dependences of the Kerr effects of ammonia, methylamine, d methylamine and trimethylamine.

made at high pressures, up to 3100 kPa, the effects of the Kerr second and third virial coefficients may be significant and this level of agreement may be coincidental.

As large errors are associated with coefficients derived from a quadratic expression, the procedure of Buckingham and Orr[16] was followed in the analysis of the temperature dependences of the Kerr effects. This involved evaluation of one of the three terms in equation 3.2 using data from other sources, followed by rearrangement of the equation into a linear form. For ammonia and trimethylamine, the optical-frequency polarizabilities, and therefore $\alpha_{zz} - \alpha$, were determined from Rayleigh light-scattering experiments;[5,6] and accurate dipole moments were obtained from laser-microwave double resonance[12] and microwave[15] spectroscopy. Equation 3.2 was then recast as

$$\left\{A_K - \left(N_A/270\varepsilon_0 k^2\right)\mu^2(\alpha_{zz} - \alpha)T^{-2}\right\} = (N_A/81\varepsilon_0)\gamma^K + (N_A/81\varepsilon_0 k)\left\{(2/3)\mu\beta^K + (9/5)\alpha\alpha^0\kappa\kappa^0\right\}T^{-1} \qquad (3.3)$$

where $(3/10)\left(\alpha_{\alpha\beta}\alpha^0_{\alpha\beta} - 3\alpha\alpha^0\right) = (9/5)\alpha\alpha^0\kappa\kappa^0$. In this first-order polynomial in T^{-1}, γ^K is proportional to the intercept and β^K is related to the gradient. As the static polarizability anisotropy parameter, κ^0, is unknown for most molecules and is not expected to possess a large dispersion, $\kappa\kappa^0$ can be approximated by κ^2. Any error in this assumption is mitigated by the small size of the $\alpha\alpha^0\kappa^2$ contribution, in the case of the methylamine series, and the fact that β^K is the only other term affected. The analyses of the Kerr effects of ammonia and trimethylamine, using this procedure, are depicted in Figures 3.2 and 3.3. It is evident that the quantities being plotted against T^{-1} in these two graphs are small compared to the Kerr first virial coefficients listed in Tables 3.1 and 3.4. As will be shown later, these quantities are only 25% and 11% of A_K for ammonia and trimethylamine at 300 K, respectively. This results in the relatively larger statistical uncertainties and scatter of the data points indicated in Figures 3.2 and 3.3, with the uncertainties for the trimethylamine data being larger than those for the analysis of the ammonia data.

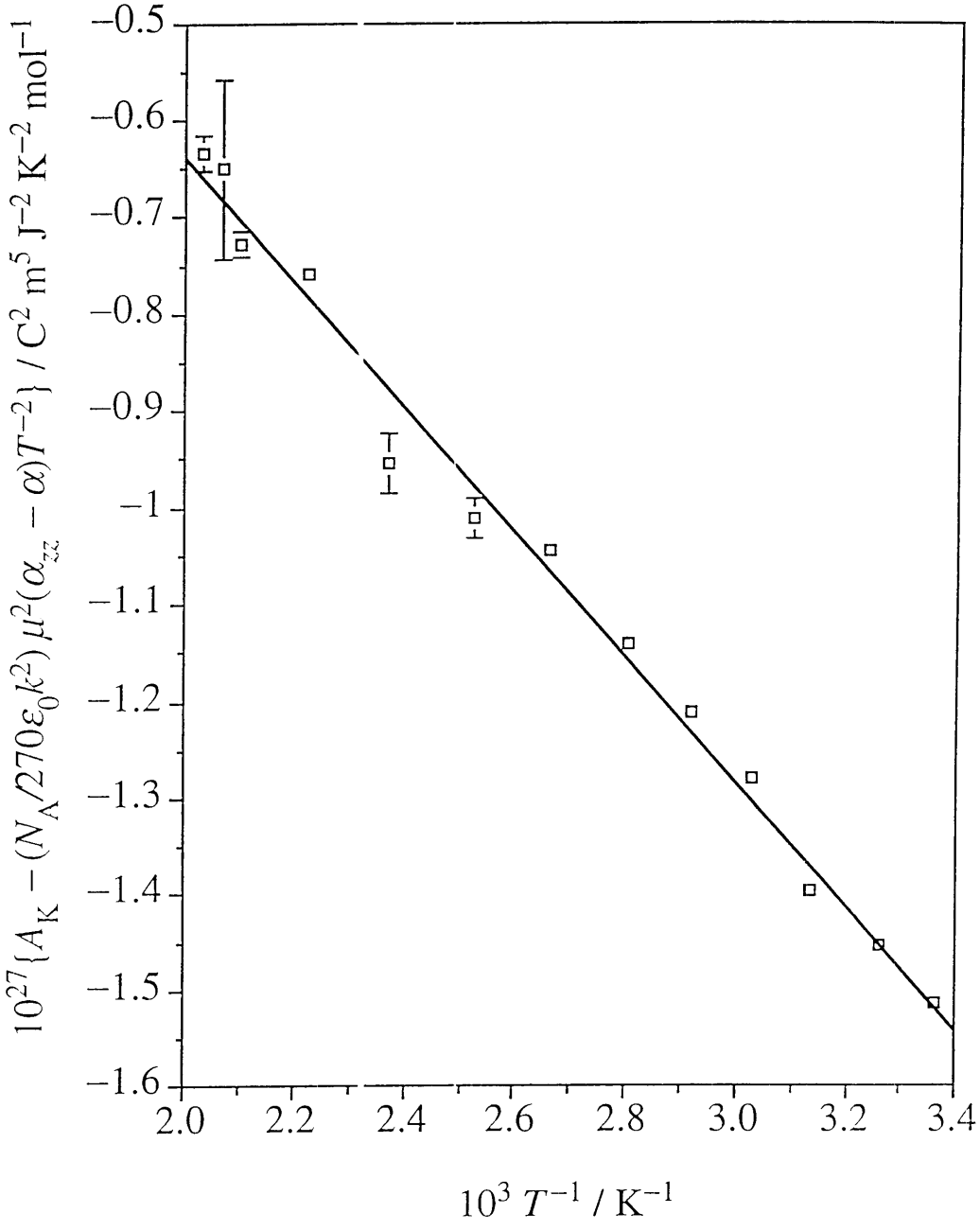

Figure 3.2 Analysis of the Kerr effect of ammonia.

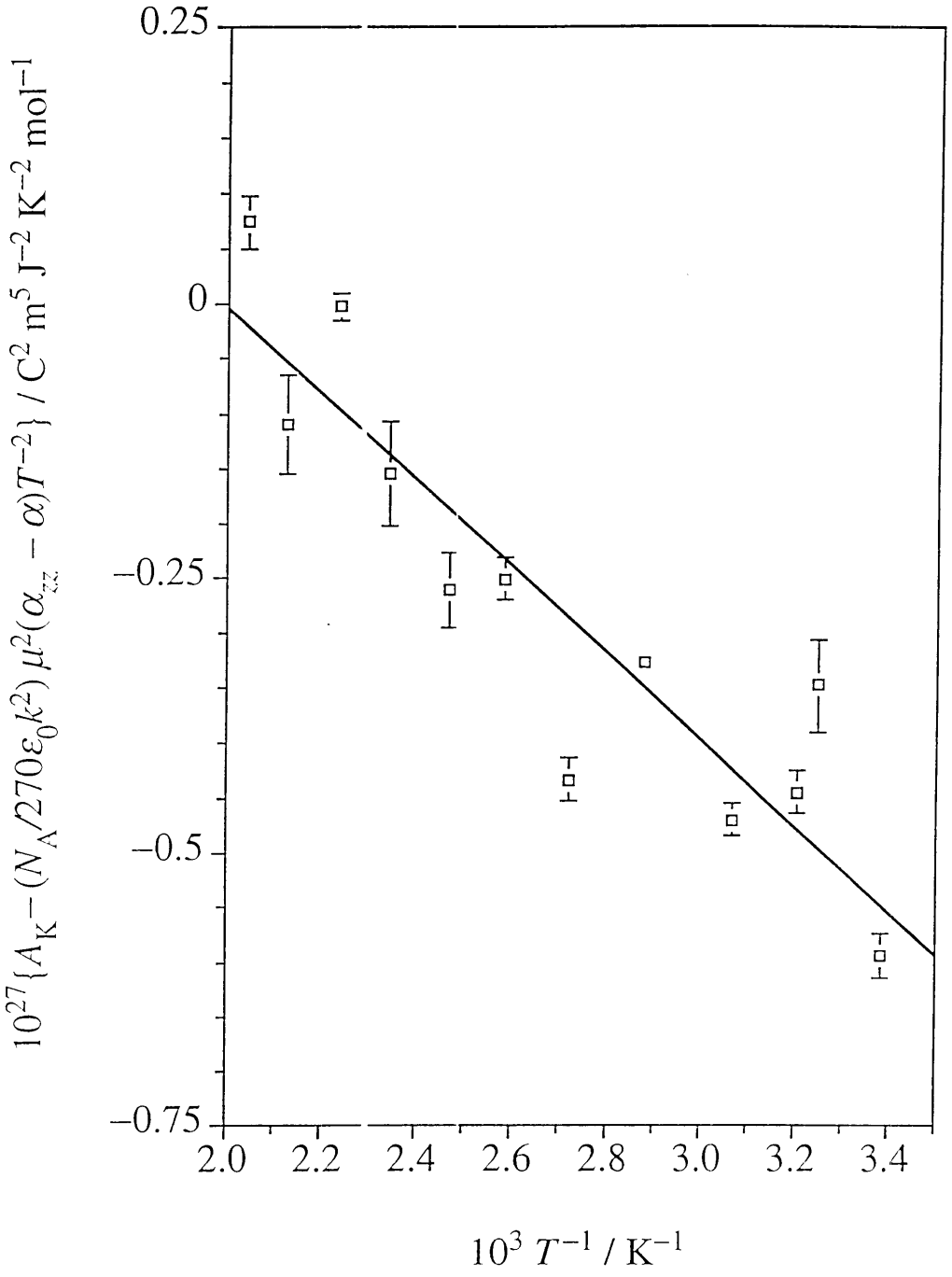

Figure 3.3 Analysis of the Kerr effect of trimethylamine.

Tables 3.5 and 3.6 list the electric properties of ammonia and trimethylamine derived from the Kerr-effect results. The orientations of the molecular axes for these two species are identical, with the z - axis being coincident with the C_3 axis and the dipole moment, and the x - and y - axes being orthogonal to each other and the C_3 axis. Bridge and Buckingham[5] derived the mean polarizability of ammonia at 632.8 nm from refractivity data. Stankey[6] measured the mean polarizability of trimethylamine at 632.8 nm, and this is in reasonable agreement with the value of $\alpha = 8.43\times10^{-40}\,C^2\,m^2\,J^{-1}$, evaluated by Burton et al.[17] at the same wavelength. Mean static polarizabilities were derived from dielectric polarization measurements,[11] and were assigned uncertainties of ± 3%.

The relative importance of the dispersion and vibrational contributions to the hyperpolarizabilities for different nonlinear optical processes is poorly characterized for even the simplest of polyatomic molecules. The value of $\gamma^{K} = (0.78\pm0.07)\times10^{-60}$ $C^4\,m^4\,J^{-3}$ for ammonia obtained in this study is twice as large as the value of $\gamma(-2\omega;0,\omega,\omega) = (0.383\pm0.007)\times10^{-60}\,C^4\,m^4\,J^{-3}$, derived from second harmonic generation measurements by Ward and Miller[7] at 694.3 nm. Bishop et al.[18] have performed calculations at the SCF level which predict the vibrational contributions to γ^{K} and $\gamma(-2\omega;0,\omega,\omega)$ for ammonia to be only 6% and −1%, respectively. Although these predictions should be treated with some caution, as they were made with a small basis set and do not take into account nuclear vibrations, the difference between γ^{K} and $\gamma(-2\omega;0,\omega,\omega)$ for ammonia may be due to dispersion. A recent coupled-cluster calculation by Sekino and Bartlett[19] predicts a value of $\gamma^{K} = (0.29\pm0.07)\times10^{-60}\,C^4\,m^4\,J^{-3}$ at 694.3 nm, which is smaller than the experimental value at 632.8 nm.

Similarly, the Kerr first hyperpolarizability for ammonia, $\beta^{K} = (-0.331\pm0.011)$ $\times10^{-50}\,C^3\,m^3\,J^{-2}$, is larger than the corresponding second harmonic generation value of $\beta(-2\omega;\omega,\omega) = (-0.157\pm0.004)\times10^{-50}\,C^3\,m^3\,J^{-2}$ at 694.3 nm.[7] As Bishop et al.[18] have predicted small vibrational contributions for the two nonlinear optical processes, 22% of the electronic component for β^{K} and 0% for $\beta(-2\omega;\omega,\omega)$, the dispersion

Table 3.5 Analysis of the Kerr effect of ammonia at 632.8 nm

Property	Value
10^{24} slope / C^2 m^5 J^{-2} K^{-1} mol^{-1} a)	−0.645 ± 0.022
10^{27} intercept / C^2 m^5 J^{-2} K^{-2} mol^{-1} a)	0.65 ± 0.06
10^{40} α / C^2 m^2 J^{-1} b)	2.47 ± 0.02
10^{40} α^0 / C^2 m^2 J^{-1} c)	2.60 ± 0.08
10^3 κ^2 b)	1.85 ± 0.12
10^{30} μ / C m d)	4.90984 ± 0.00024
10^{40} α_{xx} / C^2 m^2 J^{-1} b)	2.36
10^{40} α_{yy} / C^2 m^2 J^{-1} b)	2.36
10^{40} α_{zz} / C^2 m^2 J^{-1} b)	2.68
10^{50} β^K / C^3 m^3 J^{-2}	−0.331 ± 0.011
10^{60} γ^K / C^4 m^4 J^{-3}	0.78 ± 0.07

a) From equation 3.3. b) Reference 5. c) Reference 11. d) Reference 12.

Table 3.6 Analysis of the Kerr effect of trimethylamine at 632.8 nm

Property	Value
10^{24} slope / C^2 m^5 J^{-2} K^{-1} mol^{-1} a)	−0.47 ± 0.05
10^{27} intercept / C^2 m^5 J^{-2} K^{-2} mol^{-1} a)	1.01 ± 0.14
10^{40} α / C^2 m^2 J^{-1} b)	8.69 ± 0.09
10^{40} α^0 / C^2 m^2 J^{-1} c)	8.82 ± 0.26
10^3 κ^2 b)	1.38 ± 0.05
10^{30} μ / C m d)	2.041 ± 0.034
10^{40} α_{xx} / C^2 m^2 J^{-1} b)	9.01
10^{40} α_{yy} / C^2 m^2 J^{-1} b)	9.01
10^{40} α_{zz} / C^2 m^2 J^{-1} b)	8.04
10^{50} β^K / C^3 m^3 J^{-2}	−0.71 ± 0.06
10^{60} γ^K / C^4 m^4 J^{-3}	1.21 ± 0.17

a) From equation 3.3. b) Reference 6. c) Reference 11. d) Reference 15.

appears to be the principal difference between these two values. The coupled cluster calculation of $\beta^{K} = -0.133 \times 10^{-50}\,C^3\,m^3\,J^{-2}$ at 694.3 nm by Sekino and Bartlett[19] again underestimates the experimental value. It is evident that, even for simple polyatomic molecules, a comparison of hyperpolarizabilities measured for different nonlinear optical processes and at different wavelengths is complicated.

Even such a cursory comparison of hyperpolarizabilities is not possible for the methylated derivatives of ammonia, due to an absence of other results. This work presents the first reported hyperpolarizabilities for trimethylamine. As γ^{K} is only slightly larger for trimethylamine than for ammonia, the effect of methyl-group substitution on this property appears to be small. The Kerr second hyperpolarizability is approximately additive in nature and is amenable to bond additivity methods.[16,20,21,22] Therefore, reasonable estimates of the Kerr second hyperpolarizabilities for methylamine and dimethylamine should be obtained by interpolation from the values for ammonia and trimethylamine. Then equation 3.2 can be rewritten as

$$\left[A_K - (N_A/81\varepsilon_0)\gamma^K\right]T = (N_A/81\varepsilon_0 k)\left\{\left[(2/3)\mu\beta^K + (9/5)\alpha\alpha^0\kappa^2\right] + (3/10k)\mu^2(\alpha_{zz} - \alpha)T^{-1}\right\}. \qquad (3.4)$$

The analyses of the temperature dependences of the Kerr effects of methylamine and dimethylamine by this method are shown in Figures 3.4 and 3.5. The mean polarizabilities of these two species were measured by Rayleigh light scattering[6] at 632.8 nm and are in excellent agreement with those determined by Burton et al.[17] at the same wavelength, $\alpha = 4.47$ and $6.53 \times 10^{-40}\,C^2\,m^2\,J^{-1}$. Mean static polarizabilities were obtained from dielectric polarization data.[11]

For molecules with C_s symmetry, the direction of the dipole moment does not coincide with one of the principal axes of the polarizability. This gives rise to a fourth non-zero component of the experimentally-determined polarizability tensor. The off-diagonal component can be obtained from a combination of experiment and theory. Figure 3.6 shows the general relationship between the natural or Kerr-effect axes and the

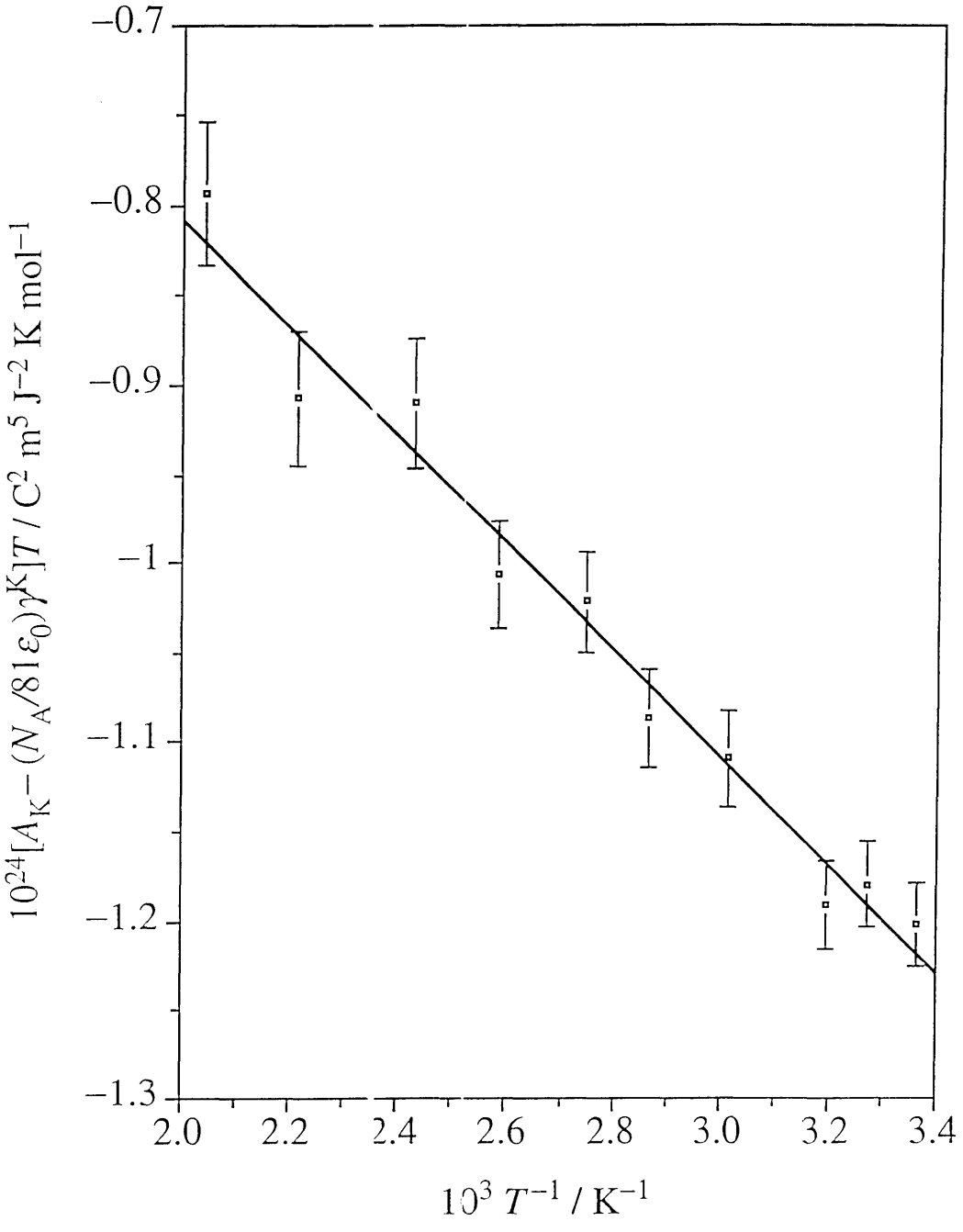

Figure 3.4 Analysis of the Kerr effect of methylamine.

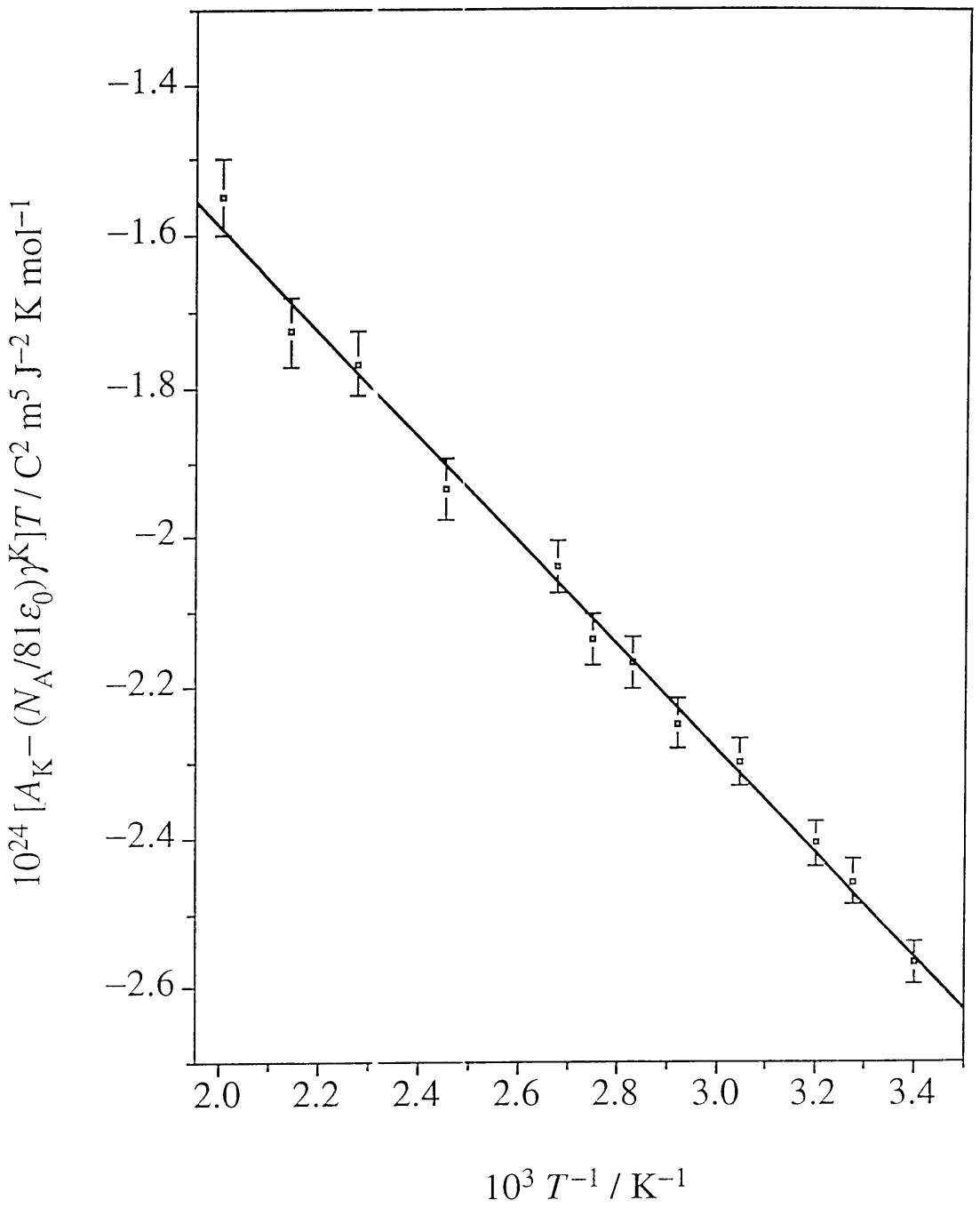

Figure 3.5 Analysis of the Kerr effect of dimethylamine.

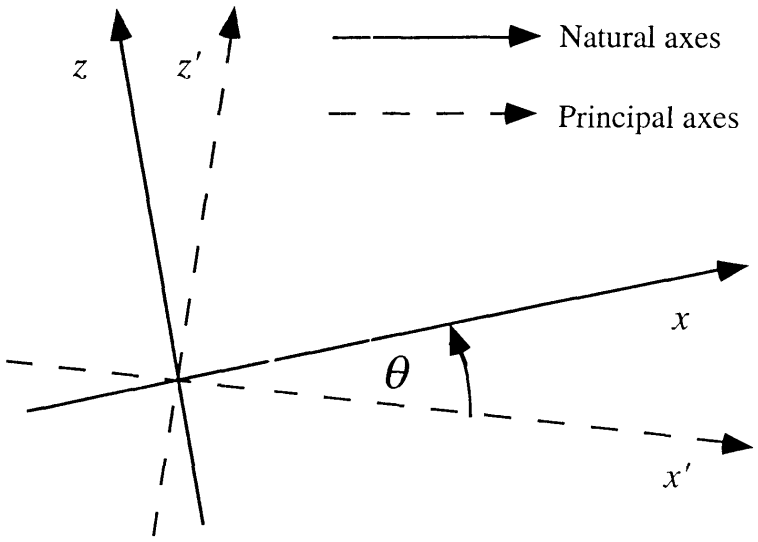

Figure 3.6 Coordinate frames for molecules with C_s symmetry.

principal axes of a molecule with C_s symmetry. The natural axes are defined by the direction of the dipole moment, and the xz and $x'z'$ planes are coincident with the mirror plane of the molecule in its equilibrium conformation, where primes refer to the principal axes. The y - and y' - axes are normal to the plane of symmetry and coincident, and the centre of mass is the origin of both sets of axes. In Figure 3.6, the y - axis is taken as positive in the direction going into the plane of the page, in order to preserve a right-handed axis system. Counterclockwise rotations around the y - axis are positive, and clockwise rotations are negative, in sign.

By definition,[23] second rank tensors transform according to

$$\alpha_{\alpha\beta} = \alpha_{\alpha'\beta'} a_{\alpha'\alpha} a_{\beta'\beta} \tag{3.5}$$

where $a_{\alpha'\alpha}$ and $a_{\beta'\beta}$ are the direction cosines. The off-diagonal component of the polarizability is then given by [24]

$$\begin{aligned} \alpha_{xz} &= \alpha_{\alpha'\beta'} a_{\alpha' x} a_{\beta' z} \\ &= \alpha_{z'z'} \sin\theta\cos\theta - \alpha_{x'x'} \sin\theta\cos\theta \\ &= \tfrac{1}{2}(\alpha_{z'z'} - \alpha_{x'x'})\sin 2\theta \end{aligned} \tag{3.6}$$

In order to relate α_{xz} to the experimental polarizabilities, $\alpha_{x'x'}$ and $\alpha_{z'z'}$ are similarly transformed into the natural axis system through

$$\begin{aligned}\alpha_{xx} &= \alpha_{\alpha'\beta'} a_{\alpha' x} a_{\beta' x} \\ &= \alpha_{x'x'} \cos^2\theta + \alpha_{z'z'} \sin^2\theta \\ &= \alpha_{x'x'} - \alpha_{x'x'} \sin^2\theta + \alpha_{z'z'} \sin^2\theta\end{aligned} \tag{3.7}$$

$$\begin{aligned}\alpha_{zz} &= \alpha_{\alpha'\beta'} a_{\alpha' z} a_{\beta' z} \\ &= \alpha_{x'x'} \sin^2\theta + \alpha_{z'z'} \cos^2\theta \\ &= \alpha_{x'x'} - \alpha_{x'x'} \cos^2\theta + \alpha_{z'z'} \cos^2\theta.\end{aligned} \tag{3.8}$$

Subtraction of equation 3.7 from equation 3.8 then gives

$$\alpha_{z'z'} - \alpha_{x'x'} = (\alpha_{zz} - \alpha_{xx})(\cos 2\theta)^{-1} \tag{3.9}$$

and substitution into equation 3.6 yields

$$\alpha_{xz} = \tfrac{1}{2}(\alpha_{zz} - \alpha_{xx}) \tan 2\theta. \tag{3.10}$$

Ab initio calculations at the second order Møller-Plesset perturbation theory (MP2) level, using a 6-31G (+sd+sp) basis set and MP2/DZP optimized goemetries, were performed by Dr M.A. Spackman on methylamine and dimethylamine.[25] The polarizabilities were first computed in the inertial axis system and then diagonalized in order to obtain the orientation of the principal axis system. The angle, θ, between the principal and natural axis systems was then determined from the known direction of the experimental dipole moment.

For molecules of C_s symmetry, equation 1.24 reduces to

$$\kappa^2 = \left(3\alpha^2 + \alpha_{xz}^2 - \alpha_{xx}\alpha_{yy} - \alpha_{xx}\alpha_{zz} - \alpha_{yy}\alpha_{zz}\right)\Big/ 3\alpha^2 \tag{3.11}$$

so that the determination of α_{xx} and α_{yy} requires knowledge of the angle θ.

Tables 3.7 and 3.8 present the first sets of polarizabilities for methylamine and dimethylamine. Figure 3.7 shows the natural and principal polarizability axis systems for the two molecules, with the plane of the page being coincident with the mirror planes of the equilibrium conformations of the molecules. The y - direction for each molecule is positive going into the plane of the page. For methylamine, the z - axis is oriented at an angle of 107.1°, and the x - axis at 17.1°, to the C-N bond.[13] The orientation of the calculated dipole moment was within 3.6° of that of the experimental dipole moment[13] and, as a consequence, the evaluation of $\theta = 20.8^{\circ}$ should be reasonably accurate. Furthermore, the effect of the value of θ on the magnitude of the derived polarizability components is generally small, as methylamine is not very anisotropic. A variation of 5° in θ was found to change α_{xx} by 1.5% and α_{yy} by 0.6%. Greater underestimates of θ for methylamine have little effect, with $\theta = 0^{\circ}$ altering α_{xx} and α_{yy} by 1% each. Overestimates of θ greater than 5° result in much larger changes, up to 11% at $\theta = 41^{\circ}$.

The derivation of α_{xx} and α_{yy} for molecules of C_s symmetry involves a quadratic equation and, therefore, two sets of polarizability components eventuate. In the case of methylamine, the tabulated set of α_{xx}, α_{yy}, α_{xz} was selected on the basis that $\alpha_{xx} > \alpha_{yy}$, as indicated by the ab initio results of Spackman.[25] These are compared with the experimental values in Table 3.9, from which it can be seen that agreement is within 5%. Equation 3.10 and the computed values of α_{xx}, α_{zz} and θ were used to determine the ab initio values of α_{xz}.

The z - axis of dimethylamine is orientated at 115.1°, and the x - axis at 25.1°, to the bisector of the C-N-C angle.[14] The angle between the principal axis system and the experimental axis system was calculated to be 37.7°.[25] However, the quadratic equation was insoluble using this value and, in view of the accuracy and consistency of the experimental data, the most probable source of error was in the calculated orientation of the principal axes. As the direction of the dipole moment determined from the MP2 calculations differed by an angle of 5.3° from that of the experimental dipole moment,[14] an angle of 32.4° was used to calculate α_{xx}, α_{yy} and α_{xz}. The polarizabilities so derived were also found to be insensitive to small changes in θ. A variation of 2.4° in

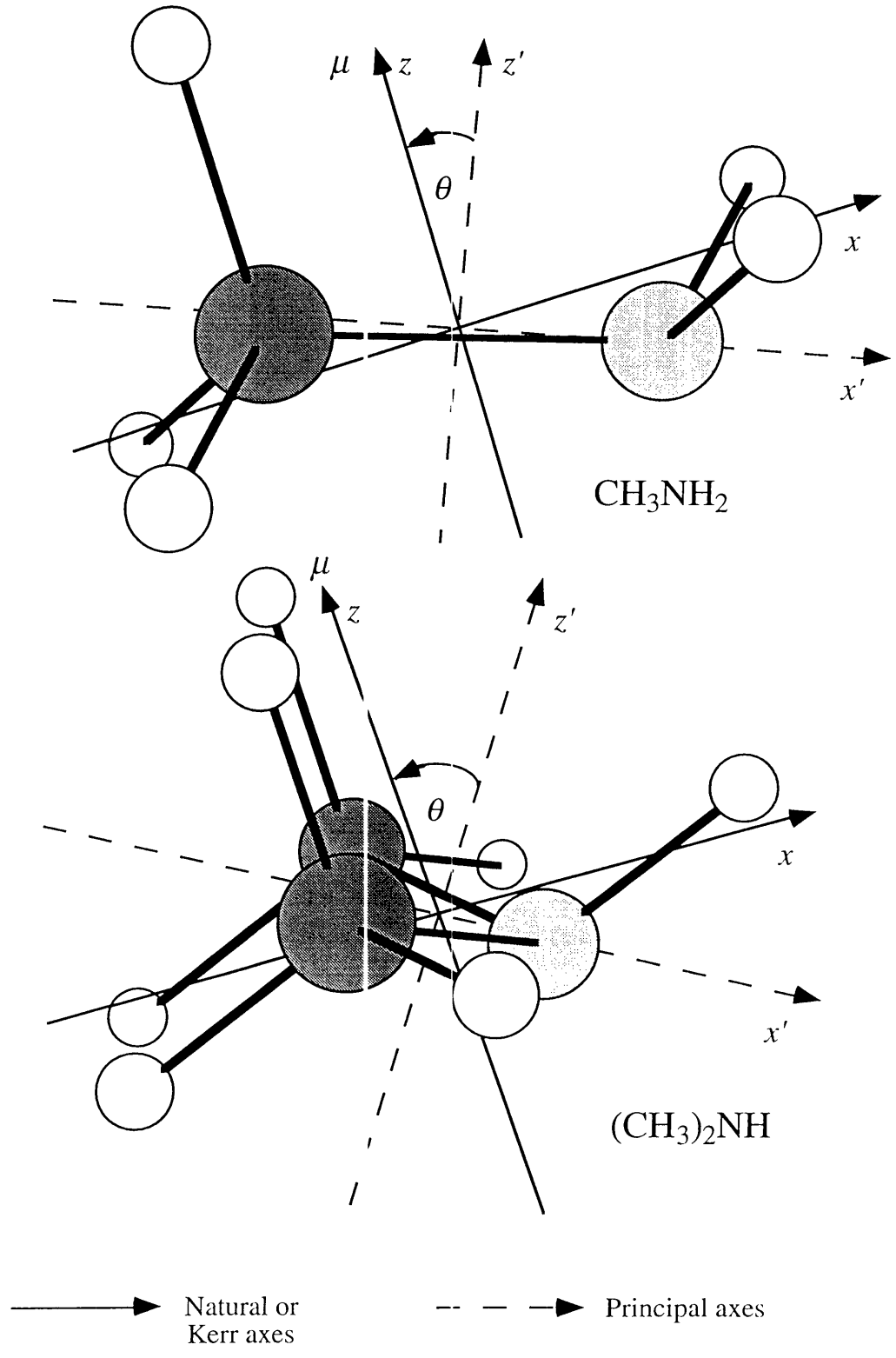

Figure 3.7 Structures and molecular axes for methylamine and dimethylamine.

Table 3.7 Analysis of the Kerr effect of methylamine at 632.8 nm

Property	Value
10^{21} slope / $C^2\ m^5\ J^{-2}\ \zeta^2\ mol^{-1}$ a)	−0.296 ± 0.017
10^{24} intercept / $C^2\ m^5\ J^{-2}\ K\ mol^{-1}$ a)	−0.22 ± 0.05
$10^{40}\ \alpha$ / $C^2\ m^2\ J^{-1}$ b)	4.53 ± 0.05
$10^{40}\ \alpha^0$ / $C^2\ m^2\ J^{-1}$ c	4.68 ± 0.14
$10^3\ \kappa^2$ b)	2.67 ± 0.17
$10^{30}\ \mu$ / C m d)	4.42 ± 0.05
$10^{60}\ \gamma^K$ / $C^4\ m^4\ J^{-3}$	0.9
θ e)	20.8°
$10^{40}\ \alpha_{xx}$ / $C^2\ m^2\ J^{-1}$	4.91 ± 0.06
$10^{40}\ \alpha_{yy}$ / $C^2\ m^2\ J^{-1}$	4.26 ± 0.10
$10^{40}\ \alpha_{zz}$ / $C^2\ m^2\ J^{-1}$	4.42 ± 0.05
$10^{40}\ \alpha_{xz}$ / $C^2\ m^2\ J^{-1}$	−0.22 ± 0.03
$10^{50}\ \beta^K$ / $C^3\ m^3\ J^{-2}$	−0.16 ± 0.03

a) From equation 3.4. b) Reference 6. c) Reference 11. d) Reference 13.

e) Reference 25.

Table 3.8 Analysis of the Kerr effect of dimethylamine at 632.8 nm

Property	Value
10^{21} slope / $C^2\ m^5\ J^{-2}\ K^2\ mol^{-1}$ a)	−0.689 ± 0.016
10^{24} intercept / $C^2\ m^5\ J^{-2}\ K\ mol^{-1}$ a)	−0.22 ± 0.05
$10^{40}\ \alpha$ / $C^2\ m^2\ J^{-1}$ b)	6.60 ± 0.07
$10^{40}\ \alpha^0$ / $C^2\ m^2\ J^{-1}$ c)	6.62 ± 0.20
$10^3\ \kappa^2$ b)	3.31 ± 0.10
$10^{30}\ \mu$ / C m d)	3.369 ± 0.034
$10^{60}\ \gamma^K$ / $C^4\ m^4\ J^{-3}$	1.1
θ e)	32.4°
$10^{40}\ \alpha_{xx}$ / $C^2\ m^2\ J^{-1}$	6.35 ± 0.36
$10^{40}\ \alpha_{yy}$ / $C^2\ m^2\ J^{-1}$	7.31 ± 0.18
$10^{40}\ \alpha_{zz}$ / $C^2\ m^2\ J^{-1}$	6.14 ± 0.07
$10^{40}\ \alpha_{xz}$ / $C^2\ m^2\ J^{-1}$	−0.22 ± 0.39
$10^{50}\ \beta^K$ / $C^3\ m^3\ J^{-2}$	−0.27 ± 0.04

a) From equation 3.4. b) Reference 6. c) Reference 11. d) Reference 14.

e) Reference 25.

Table 3.9 Comparison of the experimental and ab initio polarizabilities for methylamine and dimethylamine at 632.8 nm [a]

	CH_3NH_2		$(CH_3)_2NH$	
	This work	Ab initio [b]	This work	Ab initio [b]
α	4.53 ± 0.05	4.31	6.60 ± 0.07	6.37
α_{xx}	4.91 ± 0.06	4.69	6.35 ± 0.36	6.20
α_{yy}	4.26 ± 0.10	4.04	7.31 ± 0.18	6.99
α_{zz}	4.42 ± 0.05	4.20	6.14 ± 0.07	5.93
α_{xz}	−0.22 ± 0.03	−0.22	−0.22 ± 0.39	−0.29

a) Expressed in units of 10^{-40} C^2 m^2 J^{-1}. b) Reference 25.

θ altered α_{xx} by 0.4% and α_{yy} by 0.3%. An underestimate of greater than 15° was required to change α_{xx} and α_{yy} by more than 1%. Larger overestimates of θ, however, resulted in an insoluble quadratic equation. The polarizabilities listed in Table 3.8 were selected from the quadratic analysis after comparison with the ab initio results. Although the polarizabilities of dimethylamine were not determined as accurately as for those of methylamine, they are reasonably well described.

The hyperpolarizabilities of methylamine and dimethylamine have not been reported previously. The interpolated values for γ^K vary incrementally from those of ammonia and trimethylamine. A systematic variation of β^K for the methylamine series does not occur with successive methyl substitution, possibly because the experimental observable of β^K transforms as a vector.

The absolute and percentage contributions to A_K from the various terms for the methylamines at 300 K are listed in Table 3.10. It is clear that for each molecule the $\mu^2(\alpha_{zz} - \alpha)$ term is dominant, although there is a small decrease in the importance of

Table 3.10 Contributions of individual terms to A_K of the methylamines at 300 K [a]

Term	NH_3	CH_3NH_2	$(CH_3)_2NH$	$(CH_3)_3N$
$(N_A/81\varepsilon_0)\gamma^K$	0.65 (11.0%)	0.77 (−23.6%)	0.89 (−11.8%)	1.01 (−22.8%)
$(2N_A/243\varepsilon_0 kT)\mu\beta^K$	−2.19 (−37.0%)	−0.94 (28.8%)	−1.24 (16.5%)	−1.94 (43.5%)
$(9N_A/405\varepsilon_0 kT)\alpha\alpha^0\kappa^2$	0.04 (0.7%)	0.20 (−6.1%)	0.52 (−6.9%)	0.37 (−8.4%)
$(N_A/270\varepsilon_0 k^2T^2)\mu^2(\alpha_{zz}-\alpha)$	7.42 (125.3%)	−3.28 (100.8%)	−7.59 (100.8%)	−3.96 (89.1%)
A_K	5.92	−3.26	−7.53	−4.44

a) Expressed in units of 10^{-27} C^2 m^5 J^{-2} mol^{-1}.

this term with successive methyl-group substitution. The differences in the sign and curvature of the Kerr first virial coefficients of ammonia and trimethylamine, evident in Figure 3.1, are due to the dominance of this term. Steric repulsion between the bulky methyl groups of the trimethylamine molecule changes the molecular geometry with respect to that of ammonia. The H-N-H bond angle is 107.23° in ammonia, and the C-N-C bond angle is 110.9° in trimethylamine.[26] This reduces the α_{zz} component of the polarizability in relation to the mean polarizability, reversing the sign of the $\mu^2(\alpha_{zz}-\alpha)$ term and giving a negative Kerr constant for trimethylamine.

The contributions of the hyperpolarizability terms are also significant. The γ^K and $\mu\beta^K$ terms are opposite in sign in all four species and tend to cancel each other.

However, the magnitudes of their individual contributions, ≈10 - 40% of the observed Kerr constants, show that they cannot be neglected. As a consequence of their significant contributions and the precision of the intercepts and gradients of the graphs in Figures 3.2, 3.3, 3.4 and 3.5, the measured γ^K and β^K values have smaller relative uncertainties than those found for the majority of polyatomic molecules that have been investigated previously. For all of the methylamines, the $\alpha\alpha^0\kappa^2$ term makes the smallest contribution to A_K. Therefore, any inaccuracy in the values of α^0 used will have little effect on the derivation of β^K for each molecule.

In Figure 3.8, the experimental values of the Kerr second virial coefficient, B_K, for ammonia are presented in comparison with those predicted by the collision-induced polarizability model of Buckingham, Galwas and Liu,[27] as shown by equation 1.15. For the theoretical values, the force constants ε/k and r_0 were obtained from Hirschfelder, Curtiss and Bird[9] and the static polarizability anisotropy was approximated by the optical-frequency polarizability anisotropy. This has little effect on the theoretical values of B_K, as only the first term in equation 1.15 includes the static polarizability anisotropy, and it makes a maximum contribution of 1.6% over the temperature range shown. The fourth term, which is also independent of the mean static polarizability, is dominant and contributes at least 66 % of B_K. Therefore, a small error in α^0 will also have only a small effect on B_K.

It is interesting to note that the experimental and theoretical values of B_K are in excellent agreement between 400 and 500 K, but diverge at lower temperatures to differ by almost a factor of two at 300 K. Similar behaviour was reported for the temperature dependence of B_K for sulfur dioxide.[28] The reason for this apparent overestimation of the temperature dependence of B_K in the collision-induced model is not clear. Similarly, it is not obvious from the graph whether this divergence would increase at lower temperatures. Further measurements at much lower temperatures are required to address this matter, although these results do indicate the importance of the collision-induced polarizability to the Kerr second virial coefficient of dipolar molecules as vapours.

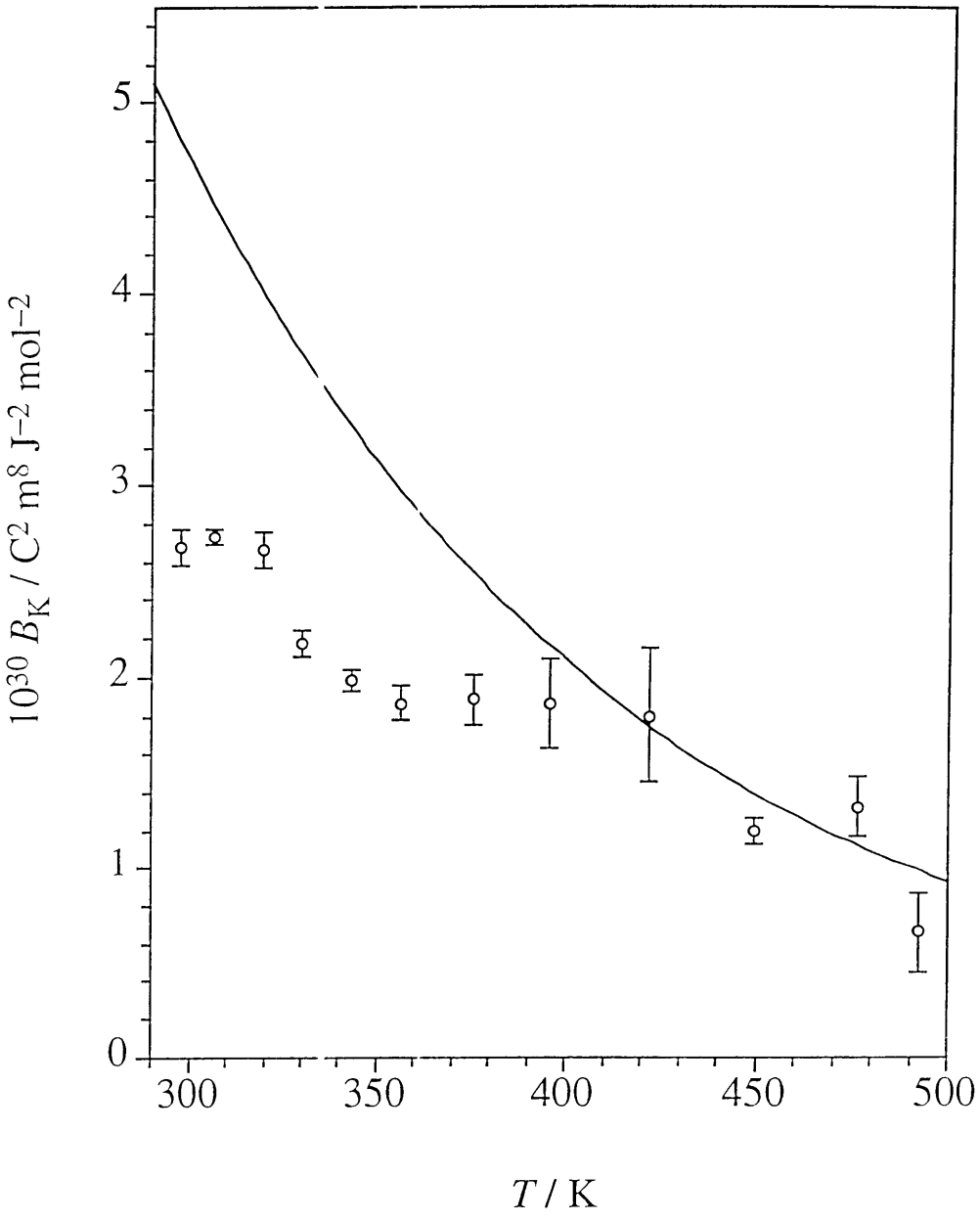

Figure 3.8 The temperature dependence of the Kerr second virial coefficient of ammonia. The values from the collision-induced polarizability model are shown by the solid line.

3.4 CONCLUSIONS

This work presents definitive experimental values of the Kerr first and second virial coefficients of ammonia, methylamine, dimethylamine and trimethylamine. Reliable polarizabilities, including the off-diagonal components, were obtained for methylamine and dimethylamine from a combination of experiment and ab initio theory. This technique is the most accurate yet reported for determining the polarizabilities of molecules with C_s symmetry. The Kerr first and second hyperpolarizabilities were also determined to a higher level of precision than has previously been reported for polyatomic molecules. The contributions of these terms to A_K were evaluated and the hyperpolarizabilities were shown to be significant for this series. Methyl-group substitution was also found to decrease the dominance of the $\mu^2(\alpha_{zz} - \alpha)$ term, and this quantity was shown to be responsible for the opposite signs of the Kerr constants of ammonia and trimethylamine. The Kerr second virial coefficients of ammonia were compared with those predicted by a collision-induced polarizability model, with the level of agreement between experiment and theory being good at high temperatures but less satisfactory at lower temperatures.

3.5 REFERENCES

1 Szivessy, G., *Z. Physik*, **26**, 323 (1924).

2 Breazeale, W.M., *Phys. Rev.*, **48**, 237 (1935).

3 Aroney, M.J. and Le Fèvre, R.J.W., *J. Chem. Soc.*, 3002 (1958).

4 Armstrong, R.S., Aroney, M.J., Calderbank, K.E. and Pierens, R.K., *Aust. J. Chem.*, **30**, 1411 (1977).

5 Bridge, N.J. and Buckingham, A.D., *Proc. Roy. Soc. A*, **295**, 334 (1966).

6 Stankey, R., *M.Sc. Thesis* (University of New England, 1991).

7 Ward, J.F. and Miller, C.K., *Phys. Rev. A*, **19**, 826 (1979).

8 Dymond, J.H. and Smith, E.B., *The Virial Coefficients of Pure Gases and Mixtures* (Clarendon Press, Oxford, 1980).

9 Hirschfelder, J.O., Curtiss, C F. and Bird, R.B., *Molecular Theory of Gases and Liquids* (Wiley, New York, 1964).

10 Lambert, J.D. and Strong, E.D.T., *Proc. Roy. Soc. A*, **200**, 566 (1950).

11 Le Fèvre, R.J.W. and Russell, P., *Trans. Faraday Soc.*, **43**, 374 (1947).

12 Tanaka, K., Ito, H. and Tanaka, T., *J. Chem. Phys.*, **87**, 1557 (1987).

13 Lide, D.R., *J. Chem. Phys.*, **27**, 343 (1957).

14 Wollrab, J.E.and Laurie, V.W., *J. Chem. Phys.*, **48**, 5059 (1968).

15 Lide, D.R. and Mann, D.E., *J. Chem. Phys.*, **28**, 572 (1958).

16 Buckingham, A.D. and Orr, B.J., *Trans. Faraday Soc.*, **65**, 673 (1969).

17 Burton, G.R., Chan, W.F., Cooper, G., Brion, C.E., Kumar, A. and Meath, W.J., *Can. J. Chem.*, **72**, 529 (1994).

18 Bishop, D.M., Kirtman, B., Kurtz, H.A. and Rice, J.E., *J. Chem. Phys.*, **98**, 8024 (1993).

19 Sekino, H. and Bartlett, R.J., *Chem. Phys. Lett.*, **234**, 87 (1995).

20 Bogaard, M.P., Orr, B.J., Buckingham, A.D. and Ritchie, G.L.D., *J. Chem. Soc., Faraday Trans. 2*, **74**, 1573 (1978).

21 Gentle, I.R. and Ritchie, G.L.D., *J. Phys. Chem.*, **93**, 7740 (1989).

22 Gentle, I.R., Hesling, M.R. and Ritchie, G.L.D., *J. Phys. Chem.*, **94**, 1844 (1990).

23 Jeffreys, H., *Cartesian Tensors* (Cambridge University Press, Cambridge, 1952).

24 Buckingham, A.D., private communication.

25 Spackman, M.A., unpublished results.

26 Landolt-Börnstein, *Numerical Data and Functional Relationships in Science and Technology*, New Series, Group II, Vol. 15 (Springer, Berlin, 1987).

27 Buckingham, A.D., Galwas, P.A. and Liu Fan-Chen, *J. Mol. Struct.*, **100**, 3 (1983).

28 Gentle, I.R., Laver, D.R. and Ritchie, G.L.D., *J. Phys. Chem.*, **94**, 3434 (1990).

CHAPTER 4 - THE KERR EFFECTS OF METHYLACETYLENE AND DIMETHYLACETYLENE

4.1 INTRODUCTION

A study of the Kerr effects of short-chain acetylenes could provide valuable insights into the influence of the carbon-carbon triple bond on the molecular polarizability and hyperpolarizabilities. Previous studies of the Cotton-Mouton effects[1,2] (the magnetic-field analogue of the Kerr effect) and the field-gradient birefringence effects[3] of the acetylenes have yielded the magnetizabilities, magnetic hyperpolarizability anisotropies and quadrupole moments of these species.

The electric properties of the parent molecule of this series, acetylene, have been investigated in a number of studies. Gas-phase Kerr-effect measurements by Buckingham et al.[4] indicated that the polarizability of acetylene is less anisotropic than that of ethylene. In addition, the Kerr second hyperpolarizability was found to be unusually large for a molecule of this size and to make a large contribution to the Kerr first virial coefficient.

The polarizabilities of the methylated derivatives of acetylene, methylacetylene and dimethylacetylene, have been characterized by Rayleigh light-scattering measurements at a number of frequencies.[5,6] A similar investigation by Keir[7] in conjunction with this work has determined the optical-frequency polarizability anisotropies of methylacetylene and dimethylacetylene. The present study was undertaken, therefore, to obtain more information about the anisotropy in the polarizability and also the Kerr second hyperpolarizabilities of methylacetylene and dimethylacetylene, to assist our efforts to determine the influence of methyl-group substitution on these properties and their relative importance to the observed Kerr constant. Kerr-effect measurements on dimethylacetylene would also provide an insight into the effect of methyl-group substitution on the static polarizability anisotropy and its relationship to the optical-frequency polarizability anisotropy for this molecule.

4.2 EXPERIMENTAL

Samples of methylacetylene (Matheson, > 96%) and dimethylacetylene (Aldrich, 99%) were found by gas chromatography to have purities of 99.99% and 99.6%, respectively, and were used without further purification.

In the case of methylacetylene, density second virial coefficients were available for the temperature range 348 - 423 K.[8] For the range 295 - 348 K, the coefficients were calculated by the same method as described for trimethylamine in Chapter 3. As the maximum vapour pressures conveniently possible were generally less than ≈ 100 kPa, any errors in these density virial coefficients will have a negligible effect on the gas densities. Measurements of the Kerr effect of methylacetylene were possible at only seven temperatures and over small pressure ranges, due to availability of only a small sample of the gas. No density second virial coefficients have been published for dimethylacetylene and so these were calculated[7] using the method of Pitzer.[9] Any errors in the gas densities, as a result of errors in these values, are likely to be small, because of the low vapour pressures that were used for dimethylacetylene.

The Kerr-effect results for methylacetylene and dimethylacetylene are listed in Tables 4.1 and 4.2. The Kerr second virial coefficients for methylacetylene were determined using a mean static polarizability obtained from the electronic contribution, found from the dispersion in the mean optical-frequency polarizability,[6] and an estimate of the vibrational contribution.[10] As no values of α^0 or α^0_{vib} have been reported for dimethylacetylene, the mean static polarizability of this species was approximated by the mean optical-frequency polarizability.

4.3 DISCUSSION

The polarizabilities of methylacetylene at 632.8 nm are known from Rayleigh light-scattering measurements and the mean polarizability.[7] Therefore, the analysis of

Table 4.1 Kerr effect of methylacetylene at 632.8 nm

T / K	Number of Pressures	Pressure Range / kPa	$10^6 B$ a) / $m^3\ mol^{-1}$	$10^{27} A_K$ / $C^2\ m^5\ J^{-2}\ mol^{-1}$	$10^{30} B_K$ b) / $C^2\ m^8\ J^{-2}\ mol^{-2}$
295.4	13	27 - 129	−412	30.19 ± 0.03	−9 ± 1
311.9	11	26 - 79	−365	27.29 ± 0.03	−6 ± 1
329.9	13	29 - 102	−321	24.67 ± 0.03	−2 ± 1
350.1	13	27 - 103	−284	22.18 ± 0.02	−3 ± 1
372.7	12	33 - 104	−244	19.98 ± 0.02	−3 ± 1
395.2	12	30 - 108	−214	18.01 ± 0.01	−4 ± 1
420.4	12	22 - 48	−184	16.35 ± 0.06	–

a) Density second virial coefficients from reference 8 and estimated values (see text). b) Calculated using $10^{40} \alpha / C^2\ m^2\ J^{-1} = 6.35 \pm 0.06$, from references 5 and 6, $10^{40} \alpha^0 / C^2\ m^2\ J^{-1} = 6.75 \pm 0.25$, from references 5 and 10, and $10^{30} \mu / C\ m = 2.6115 \pm 0.0023$, from reference 11.

Table 4.2 Kerr effect of dimethylacetylene at 632.8 nm

T / K	Number of Pressures	Pressure Range / kPa	$10^6 B$ a) / $m^3\ mol^{-1}$	$10^{27} A_K$ / $C^2\ m^5\ J^{-2}\ mol^{-1}$	$10^{30} B_K$ b) / $C^2\ m^8\ J^{-2}\ mol^{-2}$
298.2	11	24 - 48	−787	9.98 ± 0.03	6 ± 2
309.4	10	24 - 55	−725	9.72 ± 0.02	1 ± 1
322.0	10	25 - 56	−665	9.47 ± 0.02	−3 ± 1
336.4	11	25 - 71	−605	9.32 ± 0.04	−6 ± 2
352.5	12	23 - 83	−549	8.74 ± 0.02	−4 ± 1
375.2	11	21 - 57	−482	8.42 ± 0.05	−10 ± 4
397.4	11	24 - 61	−428	7.96 ± 0.03	−10 ± 2
420.1	14	23 - 55	−381	7.72 ± 0.02	−12 ± 2
442.5	11	24 - 61	−341	7.12 ± 0.02	0 ± 2
474.2	14	26 - 62	−294	6.75 ± 0.03	−2 ± 2
496.2	15	31 - 75	−267	6.67 ± 0.03	−14 ± 2

a) Density second virial coefficients from reference 7. b) Calculated using $10^{40}\alpha$ / $C^2\ m^2\ J^{-1}$ = 8.19 ± 0.08, from reference 6, and $10^{40}\alpha^0$ / $C^2\ m^2\ J^{-1}$ = 8.19 ± 0.08 (assumed value).

the Kerr-effect results for this molecule, analogously to those for ammonia and trimethylamine in Chapter 3, yields the Kerr first and second hyperpolarizabilities. Figure 4.1 shows the analysis of the Kerr-effect results for methylacetylene and Table 4.3 summarizes the results. For both methylacetylene and dimethylacetylene, the z-axis is coincident with the principal rotation axis. The dipole moment of methylacetylene was measured by Meyer et al.[11] using laser Stark spectroscopy. Even though Kerr-effect measurements for methylacetylene were possible at only seven temperatures and at low pressures, due to a shortage of sample, the accuracy and precision of these measurements are good, as indicated by Figure 4.1.

For nondipolar molecules with an axis of threefold or higher symmetry, the Kerr first virial coefficients are related to the electric properties by

$$A_K = (N_A/405\varepsilon_0)\left\{5\gamma^K + (kT)^{-1}\left(\Delta\alpha\Delta\alpha^0\right)\right\}. \tag{4.1}$$

The temperature dependence of the Kerr effect of dimethylacetylene is, therefore, expected to be linear in T^{-1}, and this is depicted in Figure 4.2. Table 4.4 presents the results for dimethylacetylene. The scatter of many of the measured Kerr constants for dimethylacetylene in Figure 4.2 is considerably larger than their statistical uncertainties. This suggests that the absolute accuracy of the Kerr-effect measurements for dimethylacetylene is less than that indicated by the precision of the Kerr first virial coefficients. The addition of a systematic uncertainty to account for this has a negligible effect on the derived electric properties. As γ^K and $\Delta\alpha\Delta\alpha^0$ would be altered by only 1% and less than 0.25%, respectively, with the addition of a 3% systematic error to the values of A_K, this was not pursued.

Although the Kerr second hyperpolarizabilities of acetylene,[4] $\gamma^K = (1.3 \pm 0.3) \times 10^{-60}$ C^4 m^4 J^{-3}, methylacetylene and dimethylacetylene make very different contributions to their respective Kerr first virial coefficients, they do show a linear correlation with methyl-group substitution. The uncertainties give a large overlap between the measured Kerr second hyperpolarizabilities for the three molecules, yet

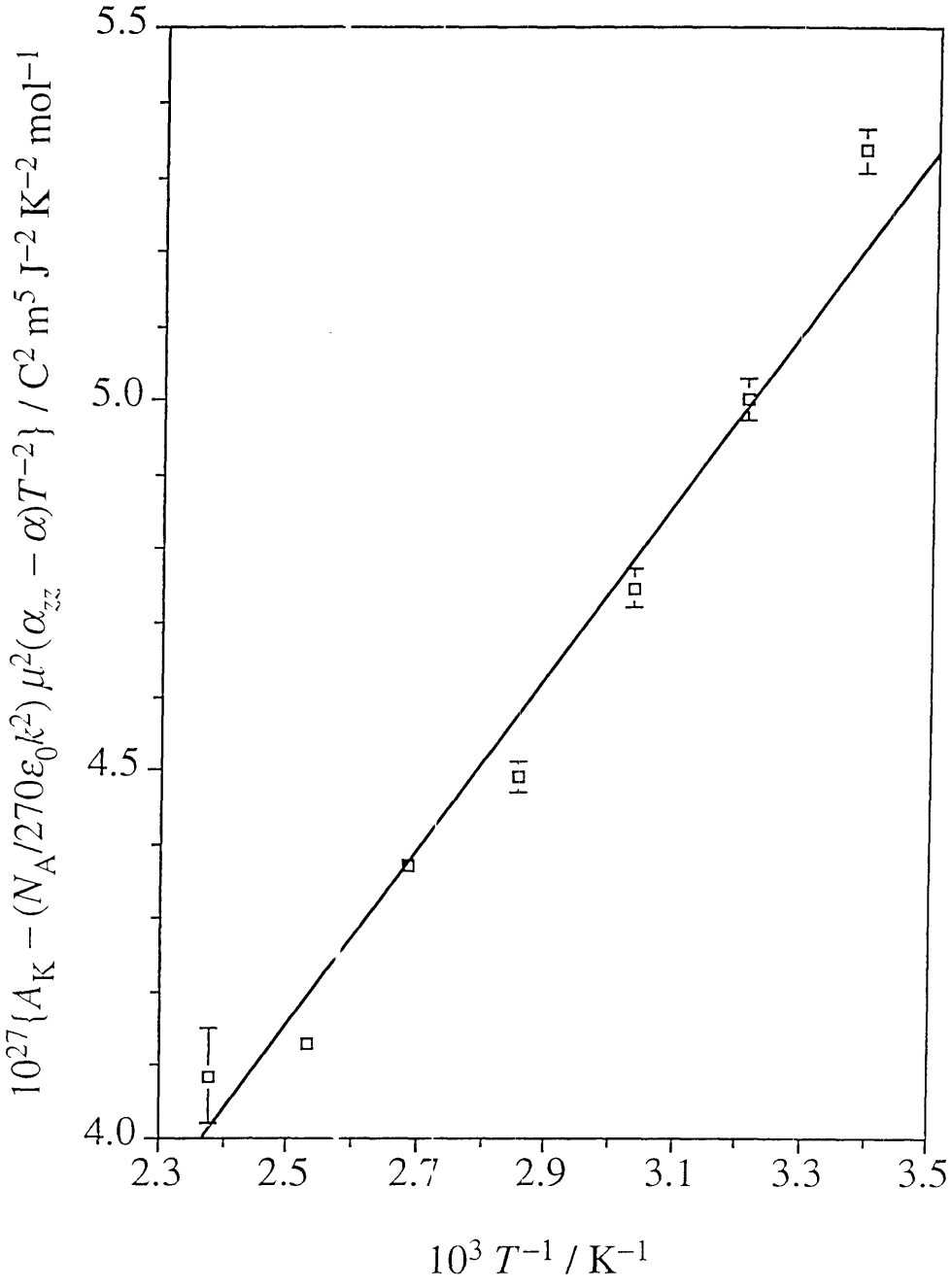

Figure 4.1 Analysis of the Kerr effect of methylacetylene.

Table 4.3 Analysis of the Kerr effect of methylacetylene at 632.8 nm

Property	Value
10^{24} slope / $C^2\ m^5\ J^{-2}\ K^{-1}\ mol^{-1}$ a)	1.18 ± 0.10
10^{27} intercept / $C^2\ m^5\ J^{-2}\ K^{-2}\ mol^{-1}$ a)	1.22 ± 0.26
$10^{40}\ \alpha$ / $C^2\ m^2\ J^{-1}$ b)	6.35 ± 0.06
$10^{40}\ \alpha^0$ / $C^2\ m^2\ J^{-1}$ c)	6.76 ± 0.25
$10^2\ \kappa^2$ d)	3.59 ± 0.10
$10^{30}\ \mu$ / C m e)	2.6115 ± 0.0023
$10^{40}\ \alpha_{xx}$ / $C^2\ m^2\ J^{-1}$	5.15 ± 0.06
$10^{40}\ \alpha_{yy}$ / $C^2\ m^2\ J^{-1}$	5.15 ± 0.06
$10^{40}\ \alpha_{zz}$ / $C^2\ m^2\ J^{-1}$	8.76 ± 0.09
$10^{50}\ \beta^K$ / $C^3\ m^3\ J^{-2}$	−0.48 ± 0.11
$10^{60}\ \gamma^K$ / $C^4\ m^4\ J^{-3}$	1.4 ± 0.3

a) From equation 3.2. b) References 5 and 6. c) References 5 and 10.

d) Reference 7. e) Reference 11.

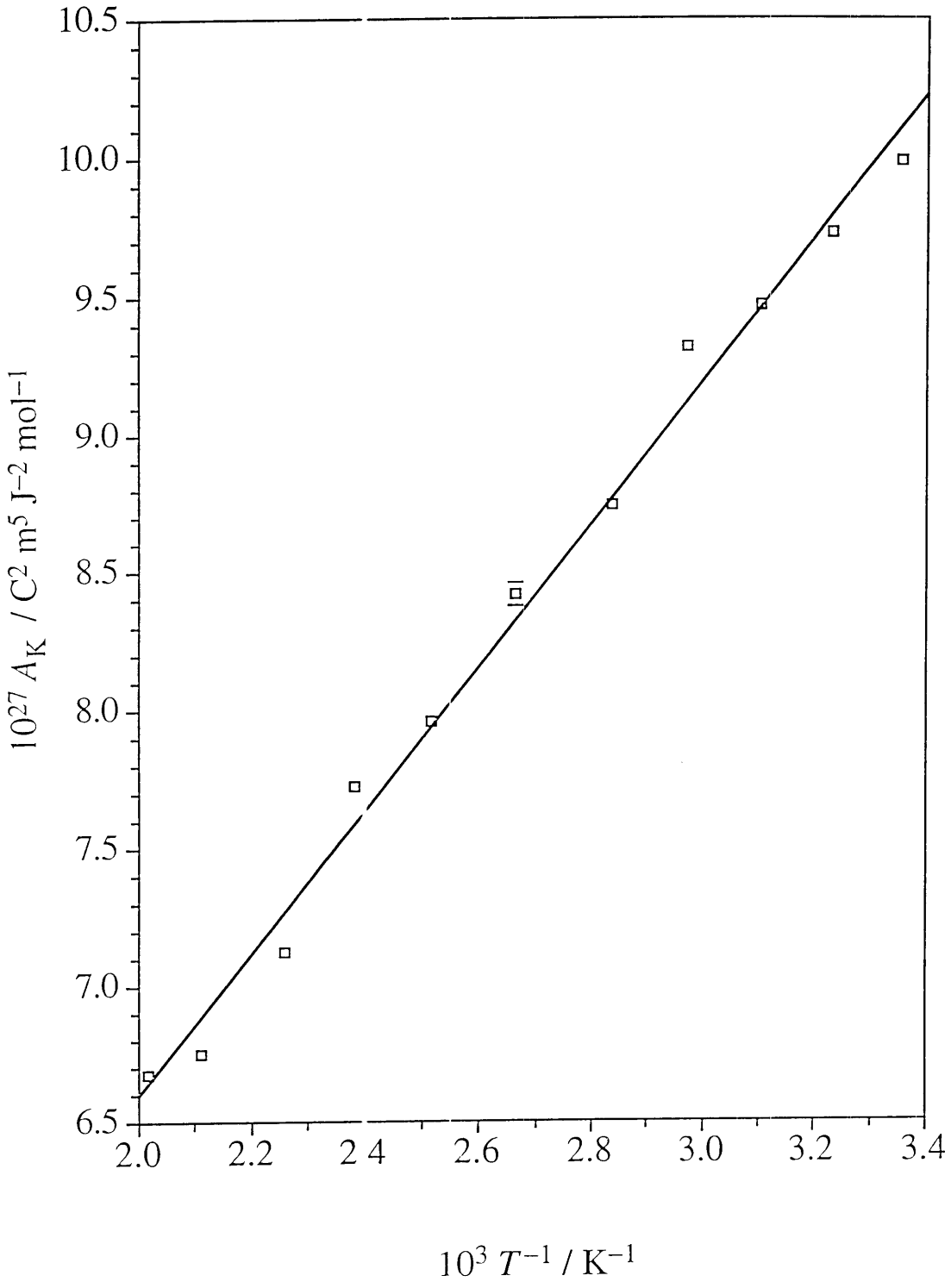

Figure 4.2 The Kerr effect of dimethylacetylene.

Table 4.4 Analysis of the Kerr effect of dimethylacetylene at 632.8 nm

Property	Value
10^{24} slope / C^2 m^5 J^{-2} K^{-1} mol^{-1} a)	2.60 ± 0.08
10^{27} intercept / C^2 m^5 J^{-2} mol^{-1} a)	1.38 ± 0.20
10^{40} α / C^2 m^2 J^{-1} b	8.19 ± 0.08
10^2 κ^2 c)	4.539 ± 0.016
10^{60} γ^K / C^4 m^4 J^{-3}	1.6 ± 0.2
10^{80} $\Delta\alpha\Delta\alpha^0$ / C^4 m^4 J^{-2} a)	21.3 ± 0.6
10^{40} $\Delta\alpha$ / C^2 m^2 J^{-1} b)	5.23 ± 0.05
10^{40} $\Delta\alpha^0$ / C^2 m^2 J^{-1}	4.08 ± 0.13

a) From equation 4.1. b) Reference 6. c) Reference 7.

Table 4.5 indicates that replacement of an acetylenic hydrogen by a methyl group increases γ^K by $\approx 0.2 \times 10^{-60}$ C^4 m^4 J^{-3}. This further supports the applicability of group additivity methods[12] for estimating γ^K.

This work presents the first reported value of the first hyperpolarizability for methylacetylene for any nonlinear optical process. Although the $\mu\beta^K$ term makes only a small contribution to A_K, as shown in Table 4.6, β^K is measured to an acceptable level of precision ($\approx \pm 20\%$). The mean static polarizability was derived from the dispersion in the optical-frequency polarizability of methylacetylene,[5] combined with an

Table 4.5 Electric properties der ved from the Kerr-effect measurements for the acetylene series

Property	HC≡CH	$CH_3C{\equiv}CH$	$CH_3C{\equiv}CCH_3$
$10^{60}\ \gamma^K$ / $C^4\ m^4\ J^{-3}$	1.3 ± 0.3 [a]	1.4 ± 0.3	1.6 ± 0.2
$\Delta\alpha^0/\Delta\alpha$	0.71 ± 0.15 [a]	–	0.78 ± 0.03

a) Reference 4.

Table 4.6 Contributions of indivi lual terms to A_K for the acetylene series at 300 K [a]

Term	HC≡CH	$CH_3C{\equiv}CH$	$CH_3C{\equiv}CCH_3$
$(N_A/81\varepsilon_0)\gamma^K$	1.07 (46%)	1.2 (4%)	1.4 (14%)
$(2N_A/243\varepsilon_0 kT)\mu\beta^K$	–	−1.7 (−6%)	–
$(9N_A/405\varepsilon_0 kT)\alpha\alpha^0\kappa^2$	1.23 (54%)	5.6 (19%)	8.6 (86%)
$\left(N_A/270\varepsilon_0 k^2T^2\right)\mu^2(\alpha_{zz}-\alpha)$	–	24.1 (82%)	–
A_K	2.30	29.3	10.0

a) Expressed in units of $10^{-27}\ C^2\ m^5\ J^{-2}\ mol^{-1}$.

estimate of the vibrational contrib ıtion from infrared intensity data.[10] The uncertainty assigned to this value of α^0 is (erived from an assumed ± 1% uncertainty in the electronic contribution and an overall uncertainty of ± 40% for the vibrational contribution. This value for the st ıtic polarizability was considered to be more reliable than the one obtained from dielectı ic polarization measurements by Watson et al.[13] The methylacetylene sample used in the earlier study[13] was stated to be impure, and the measured dipole moment was 4% lower than that determined by laser Stark spectroscopy.[11]

From the gradient in Fig ıre 4.2, the product $\Delta\alpha\Delta\alpha^0$ was found to be $(2.13 \pm 0.06) \times 10^{-79}$ C^4 m^4 J^{-2} fo dimethylacetylene. The optical-frequency and static polarizability anisotropies were separa:ed using the polarizability anisotropy at 632.8 nm, as obtained from Ray eigh light-scattering measurements.[7] Alms et al.[5] extrapolated their Rayleigh light-scattering results for dimethylacetylene at several frequencies to zero frequency, to obtain the electronic contribution to the static polarizability anisotropy. Their val ıe of 4.70×10^{-40} C^2 m^2 J^{-1} appears at first to be in only fair agreement with the static polarizability anisotropy obtained in this work, $\Delta\alpha^0 = (4.08 \pm 0.13) \times 10^{-40}$ C^2 m^2 J^{-1}. Keir's results[7] indicate that the value reported by Alms et al. is a little high. Furthermore, the vibrational contribution to the static polarizability anisotropy of dim thylacetylene is unknown. However, integrated infrared intensities[10] h ıve been used to give an estimate of $\Delta\alpha^0_{vib} = -0.82 \times 10^{-40} C^2\ m^2\ J^{-1}$ for methylacetylene. The accuracy of this value is probably not high, due to reliance upon the harmonic oscillator model. In addition, $\Delta\alpha^0_{vib}$ for dimethylacetylene wi l not necessarily bear any close similarity to the corresponding value for methylac tylene. However, this result does suggest that the vibrational contribution to the stat c polarizability anisotropy for dimethylacetylene is negative in sign and that there is reasonable agreement with the work of Alms et al.

Due to the dispersion in the electronic contribution to $\Delta\alpha$ and the contribution of the vibrational states to $\Delta\alpha^0$, the static and optical-frequency polarizability anisotropies are not necessarily similar, as shown in Table 4.5. A significant disparity is found for

dimethylacetylene, where $\Delta\alpha^0/\Delta c = 0.78 \pm 0.03$. This is in good agreement with the ratio found for acetylene by Buckingham et al.,[4] $\Delta\alpha^0/\Delta\alpha = 0.71 \pm 0.15$, although the large relative uncertainty of the latter result prevents a definitive comparison. The imprecision of this value was due to the limited pressure ranges used by the authors, for safety reasons. The authors also estimated a value of $\Delta\alpha^0$ for acetylene, with the vibrational component being obtained from a summation over the integrated infrared intensities. Although the dispersion in the electronic contribution was neglected, their derived value of $\Delta\alpha^0/\Delta\alpha = 0.68$ for acetylene further indicates that the presence of the methyl groups in dimethylacetylene tends to increase $\Delta\alpha^0$ slightly with respect to $\Delta\alpha$.

Table 4.6 lists the contributions to the Kerr first virial coefficients of acetylene, methylacetylene and dimethylacetylene at 300 K. The results for acetylene are taken from reference 4. For nondipolar molecules, the $\Delta\alpha\Delta\alpha^0$ term in equation 4.1 is equivalent to the $\alpha\alpha^0\kappa^2$ term. The contributions of the terms containing the dipole moment to the Kerr constant of methylacetylene prevent a definitive comparison of trends across the series. It is apparent, though, that the successive addition of methyl groups decreases the relative contribution of the γ^K term to the Kerr constant with respect to the $\alpha\alpha^0\kappa^2$ term. A comparison of the contributions also shows that the γ^K term makes a significant contribution to the molar Kerr constant of the nondipolar species, acetylene and dimethylacetylene. In the case of the dipolar molecule methylacetylene, however, the two hyperpolarizability terms are small and opposite in sign, with the nett result being an almost negligible contribution.

The measured Kerr second virial coefficients for methylacetylene and dimethylacetylene are uncertain, due to the low pressures used in the density-dependence studies. A comparison of these values with the collision-induced polarizability model[14] was not possible, due to the lack of force constants for these species. We can observe, however, that B_K for dimethylacetylene is positive at room temperature, is zero at approximately 310 K and generally becomes more negative as the temperature increases. This contrasts with the results for methylacetylene, for which B_K is negative at room temperature and becomes less negative at higher temperatures. A reliable value of B_K

was not obtained for the measurement on methylacetylene at 420.4 K, due to the limited pressure range. Further work on these compounds is obviously required to provide a better understanding of the behaviour of B_K in this series.

4.4 CONCLUSIONS

Accurate measurements of the Kerr first virial coefficients of methylacetylene and dimethylacetylene have yielded reasonably precise values of the hyperpolarizabilities for these species. Furthermore, the Kerr second hyperpolarizabilities of acetylene, methylacetylene and dimethylacetylene show an approximately linear correlation with methyl-group substitution, despite the very different contributions this term makes to the Kerr first virial coefficients of these molecules. These results verify the usefulness of group-additivity models in describing the effect of the methyl group on the Kerr second hyperpolarizability, which is small compared to the contribution of the triple bond. Methyl group substitution also appears to enhance the contribution of the $\alpha\alpha^0\kappa^2$ term in comparison to that of the γ^K term, and to give a small increase in the value for the static polarizability anisotropy in comparison to the polarizability anisotropy at 632.8 nm.

4.5 REFERENCES

1 Coonan, M.H. and Ritchie, G.L.D., *Chem. Phys. Lett.*, **202**, 237 (1993).

2 Lamb, D.W. and Ritchie, G.L.D., unpublished results.

3 Watson, J.N., *Ph.D. Thesis* (University of New England, 1995).

4 Buckingham, A.D., Bogaard, M.P., Dunmur, D.A., Hobbs, C.P. and Orr, B.J., *Trans. Faraday Soc.*, **60**, 1548 (1970).

5 Alms, G.R., Burnham, A.K. and Flygare, W.H., *J. Chem. Phys.*, **63**, 3321 (1975).

6 Bogaard, M.P., Buckingham, A.D., Pierens, R.K. and White, A.H., *J. Chem. Soc., Faraday Trans. I*, **74**, 3008 (1978).

7 Keir, R.I., *Ph.D. Thesis* (University of New England, 1995).

8 Dymond, J.H. and Smith, E.B., *The Virial Coefficients of Pure Gases and Mixtures* (Clarendon Press, Oxford, 1980).

9 Pitzer, K.S., *J. Am. Chem. Soc.*, **77**, 3427 (1955).

10 Bishop, D.M. and Cheung, L.M., *J. Phys. Chem. Ref. Data*, **11**, 119 (1982).

11 Meyer, F., Dupre, J., Meyer, C., Lahaye, J.G. and Fayt, A., *Can. J. Phys.*, **63**, 1184 (1985).

12 Buckingham, A.D. and Orr, B.J., *Trans. Faraday Soc.*, **65**, 673 (1969).

13 Watson, H.E., Kane, G.P. and Ramaswamy, K.L., *Proc. Roy. Soc. (London)*, **A156**, 130 & 144 (1936).

14 Buckingham, A.D., Galwas, P.A. and Liu Fan-Chen, *J. Mol. Struct.*, **100**, 3 (1983).